HHS Public Access

Author manuscript

Curr Top Med Chem. Author manuscript; available in PMC 2021 June 10.

Published in final edited form as:

Curr Top Med Chem. 2021 ; 21(2): 92–114. doi:10.2174/1568026620666201126162945.

Computational and Experimental Approaches to Investigate Lipid Nanoparticles as Drug and Gene Delivery Systems

Chun Chan[#1], **Shi Du**[#2], **Yizhou Dong**[2,3,*], **Xiaolin Cheng**[1,4,*]

[1]Division of Medicinal Chemistry and Pharmacognosy, College of Pharmacy, The Ohio State University, Columbus, OH 43210, USA;

[2]Division of Pharmaceutics and Pharmacology, College of Pharmacy, The Ohio State University, Columbus, OH 43210, USA;

[3]Department of Biomedical Engineering; The Center for Clinical and Translational Science; The Comprehensive Cancer Center; Dorothy M. Davis Heart & Lung Research Institute; Department of Radiation Oncology, The Ohio State University, Columbus, OH 43210, USA;

[4]Biophysics Graduate Program, Translational Data Analytics Institute, The Ohio State University, Columbus, OH 43210, USA

[#] These authors contributed equally to this work.

Abstract

Lipid nanoparticles (LNPs) have been widely applied in drug and gene delivery. More than twenty years ago, Doxil™ was the first LNPs-based drug approved by the US Food and Drug Administration (FDA). Since then, with decades of research and development, more and more LNP-based therapeutics have been used to treat diverse diseases, which often offer the benefits of reduced toxicity and/or enhanced efficacy compared to the active ingredients alone. Here, we provide a review of recent advances in the development of efficient and robust LNPs for drug/gene delivery. We emphasize the importance of rationally combining experimental and computational approaches, especially those providing multiscale structural and functional information of LNPs, to the design of novel and powerful LNP-based delivery systems.

Keywords

Lipid nanoparticle; Drug delivery; Gene delivery; Multiscale molecular simulation; Molecular dynamics; Machine learning

[*]Address correspondence to these authors at the Division of Pharmaceutics and Pharmacology, College of Pharmacy, The Ohio State University, Columbus, OH 43210, USA; Department of Biomedical Engineering; The Center for Clinical and Translational Science; The Comprehensive Cancer Center; Dorothy M. Davis Heart & Lung Research Institute; Department of Radiation Oncology, The Ohio State University, Columbus, OH 43210, USA; dong.525@osu.edu and Division of Medicinal Chemistry and Pharmacognosy, College of Pharmacy, The Ohio State University, Columbus, OH 43210, USA; Biophysics Graduate Program, Translational Data Analytics Institute, The Ohio State University, Columbus, OH 43210, USA; cheng.1302@osu.edu.

CONFLICT OF INTEREST

The authors declare no conflict of interest, financial or otherwise.

1. INTRODUCTION

An ideal drug delivery system (DDS) would not only protect its payloads before reaching the target site but also act as a bridge facilitating the drug's delivery into target cells. Lipid-based nanoparticles (LNPs) have attracted much attention due to their ability to encapsulate and transport small molecule drugs as well as nucleic acid drugs, their versatility in structure and composition, and their inherent selectivity towards tumor cells and inflammation sites [1,2]. For the benefits of reduced toxicity and enhanced efficacy, LNPs-based formulations of several conventional small molecule drugs have received clinical approval or have been in clinical trials for the treatment of life-threatening or even incurable diseases [3]. In addition to being a carrier for small molecule drugs, LNPs have also stirred strong interest in their application in gene therapy. LNPs have proven to be effective delivery vectors for nucleic acid drugs, and many LNPs are entering the pipeline. Since the realization of the first nanomedicine delivery system, from concept to clinical application, lipid-based DDSs have become a versatile technological platform with considerable clinical acceptance.

LNPs represent a class of nanoscale particles composed of various types of lipid components. The size and structure of LNPs may vary depending on the lipid compositions and ratios as well as the preparation methods. While empirical, combinatorial chemistry-based approaches have been widely used to develop LNPs [4], we have limited the scope of this review to the rational design of LNPs with state-of-the-art computational and experimental techniques, such as the structure-activity relationship (SAR)-based approaches. We will first review research leading to the development of LNPs for encapsulating small molecules and nucleic acids for drug delivery. To establish a structure-based framework for LNP formulation design, we will then discuss the common experimental and computational approaches to study and characterize LNPs. We will focus on computational studies that have not only elucidated the structural properties of LNPs, but also provided insights into the dynamics of LNPs as well as how LNPs interact with various endogenous molecular components during drug delivery. Lastly, by highlighting several exemplary studies that have combined experiments with computer simulation to develop novel LNP-based therapies, we conclude that a highly integrative multiscale approach will be critical for the future rational design of more efficient and robust LNP systems.

2. DEVELOPMENT OF LNPs

In the early 1960s, it was found that the dried lecithin could form a structure similar to cell membranes after hydration. Based on this observation, Bangham and Horne published electron microscope images of multilamellar vesicles, which are generally considered as the prototype of LNPs [5]. In 1965, Bangham *et al.* further studied ion diffusion through these liquid-crystalline phospholipid structures, which laid the foundation for LNPs as a DDS [6]. In the year 1968, Sessa and Weissmann successfully built a lysosomal model and defined vesicles composed of one or more layers of phospholipids as "liposome" [7]. After these early studies and in the last five decades, the development of LNPs has spurred tremendous interest in drug delivery. Nowadays, LNPs have grown into a promising biocompatible and biodegradable platform for small molecule and nucleic acid delivery.

LNPs, as a general term, refer to nanoparticles mainly constructed with lipids. Among them, liposomes are one of the most extensively studied lipid-based DDSs. Liposomes are defined as spherical vesicles consisting of single or multiple lipid bilayers, the size of which typically ranges from 50 nm to 200 nm. Liposomes can be divided into unilamellar vesicles and multilamellar vesicles (MLVs) according to the number of bilayers. Further, unilamellar liposomes are divided into small and large unilamellar vesicles (SUVs and LUVs) [8]. Besides liposomes, some LNPs are constructed with lipid-drug aggregates or other functional lipids and these lipid derivatives could spontaneously assemble into thermodynamically stable micelle-like structures [9,10]. In addition, hybrid LNPs can be prepared by introducing polymers or lipid-polymer conjugates into the systems [11–13]. Basically, lipids and their derivatives with various physiochemical and biological properties can be synthesized and used to develop LNPs for specific therapeutic applications. This flexibility of lipid-drug combinations has led to a diverse range of LNPs.

Since Doxil™ was approved by the US Food and Drug Administration (FDA) in 1995, LNPs based formulations have been applied to the treatment of diverse diseases [14]. In addition to cancer treatment (such as ovarian cancer, breast cancer, AIDS-related Kaposi's sarcoma, multiple myeloma, acute lymphoblastic leukemia), LNPs are also clinically used in antifungal therapy, antibacterial therapy, pain management, and vaccines [15]. To date, LNPs have been FDA approved for the delivery of eleven small molecule drugs, including amikacin, cytarabine, doxorubicin, bupivacaine, mifamurtide, irinotecan, paclitaxel, verteporfin, octafluoropropane, vincristine, and amphotericin B [16].

Concurrently, with the advances in LNPs for small molecule drug delivery, LNPs have been intensively explored for nucleic acid delivery [17–21]. Early studies of nucleic acid encapsulation in LNPs were reported in the late 1970s, while in these studies, the neutral lipids and passive drug loading methods resulted in poor encapsulation efficiency [22–24] [25,26]. In 1987, the application of cationic lipids, such as 2,3-bis[oleyl]oxipropyltrimethylammonium chloride (DOTMA) greatly improved the encapsulation efficiency of nucleic acid drugs due to the favorable interactions between the positively charged lipids and the negatively charged phosphate groups of nucleic acids [27]. However, the high density of charges on the surface of cationic lipids may interact with serum proteins and induce strong immune responses [28,29]. Later on, researchers investigated ionizable lipids with their apparent pKa values below 7, which ensure efficient encapsulation of nucleic acids at low pH environment, nearly neutral under the physiological pH condition in circulation, and positive surface charges at the endosomal pH [30]. In 2018, the FDA approved the clinical use of LNP-based small interfering RNA (siRNA) drug, ONPATTRO™ (Patisiran), for the treatment of polyneuropathy in adults with hereditary transthyretin-mediated amyloidosis [31]. The clinical usage of Patisiran represents significant progress in the development of LNPs for nucleic acid drug delivery. With the development of new lipids and formulations, a growing number of LNPs are ongoing in preclinical studies and clinical trials [32,33].

3. COMPOSITIONS OF LNPs

Phospholipids are the main component of biomembranes as well as LNPs, which give rise to structural integrity [34][35–37]. Phospholipids typically contain a hydrophilic moiety and two hydrophobic tails (usually alkyl chains of 14 to 18 carbons). In solution, phospholipids tend to interact with other membrane components such as cholesterol to form a continuous bilayer sheet with a thickness of 3–6 nm. Also, some phospholipids could facilitate transmembrane transport of nucleic acid payloads. For example, dioleoyl phosphatidylethanolamine (DOPE) is a neutral phospholipid composed of an amino headgroup and two oleic chains. This structure favors a non-bilayer hexagonal phase, which promotes membrane fusion, thus facilitating endocytosis and endosomal escape of nucleic acids [38]. Although the specific compositions and ingredients of individual LNPs may vary, most pharmaceutical LNPs use natural phospholipids and/or their synthetic derivatives. Currently, therapeutic LNPs approved in the clinic usually contain phosphatidylcholine (PC; neutral charge) as the main composition. Despite the diversity of lipid species in mammalian cell membranes, LNPs based products contain only one or two types of phospholipids to simplify the particle formulation and scale-up production [39].

Attempts have been made to encapsulate nucleic acids, such as plasmid DNA (pDNA) into liposomes, whereas low encapsulation rate and delivery efficiency have limited their applications in nucleic acid drug delivery. Thus, cationic lipids were introduced due to their favorable electrostatic interactions with the negatively charged nucleic acids [40]. Cationic lipids consist of a hydrophilic head group and a hydrophobic domain connected *via* a linker. The head group mostly contains amine groups, such as quaternary ammoniums, guanidiniums, heterocyclic compounds, and amino-acid derivatives [41–45]. It is not fully understood how cationic lipids facilitate the delivery of nucleic acids. One hypothesis is that the positive charges on the surface of LNPs mediate the interactions of LNPs with the negatively charged cell membrane so that nucleic acids are able to enter cells through endocytosis [46]. The hydrophobic tails of LNPs are mainly aliphatic hydrocarbon chains or cholesterol rings. The length of the aliphatic hydrocarbon chain is usually 12 to 18 carbon atoms, providing sufficient fluidity and rigidity to the lipid membrane. To a large extent, the linker determines the chemical stability and biodegradability of cationic based LNPs [47]. Recently, Ramishetti *et al.*, found that linker moieties could influence the siRNA delivery efficiency by tuning the pKa value of LNPs [48]. The effects of the hydrophobic tails, hydrophilic head groups, and linkers of cationic lipids on the delivery efficiency have been extensively reviewed in the literature [47,49,50].

Although efficient in nucleic acids encapsulation, cationic lipids have certain disadvantages, such as potentially high toxicity and immunogenicity. Animal studies showed that intravenously injected cationic liposomes caused strong interferon-γ response and liver damages [51,52]. Afterward, ionizable lipids have been used for nucleic acids delivery [30]. The apparent pKa value of ionizable lipids is less than 7, therefore, under low pH conditions, LNPs carry positive surface charges, which are beneficial to their electrostatic interaction with negatively charged nucleic acids, while at physiological pH, LNPs maintain a neutral surface charge. For example, ionizable lipids, such as 1,2-dioleoyl-3-dimethylammonium propane (DODAP) and 1,2-dioleyloxy-N,N-dimethyl-3-aminopropane (DODMA), have

been reported to carry near-neutral charge in the circulation, which has significantly increased the half-life in circulation after intravenous administration [30,53,54]. By modifying the hydrophilic head group, Jayaraman *et al.*, adjusted the pKa value of the ionizable amino lipid and studied the relationship between the pKa value and the ability to deliver siRNA. The study showed that the lipid pKa value is an important molecular factor governing siRNA delivery and the pKa of 6.2–6.5 is the optimal range for siRNA delivery *in vivo* [55]. In another study, Alabi *et al.*, further confirmed the strong correlation between the pKa of LNPs and the gene-silencing efficacy [56]. Besides nucleic acid payloads, LNPs are also explored for the delivery of Cas9/sgRNA ribonucleoprotein complexes (RNPs). For example, Wang *et al.*, developed bio-reducible LNPs for the delivery of RNPs and Cre re-combinase, respectively [57]. These LNPs induced significant gene editing both *in vitro* and *in vivo*. Recently, Wei *et al.* introduced cationic lipids (1,2-dioleoyl-3-trimethylammonium-propane [DOTAP]) into ionizable lipid 5A2-SC8 LNPs (mDLNPs). The combination of cationic lipids and ionizable lipids not only facilitated the encapsulation of RNPs but also retained the delivery capabilities of ionizable LNPs [58]. More recently, Cheng *et al.*, utilized cationic lipids to adjust the internal charge of ionizable lipid LNPs for selective organ delivery of mRNA and RNPs. A series of Selective Organ Targeting (SORT) LNPs was prepared by introducing DOTAP into mDLNPs. The SORT LNPs showed selective delivery to liver, spleen, and lung tissues when the molar ratio of DOTAP was 0%, 10–15%, and 50%, respectively [59].

In addition to phospholipids and charged lipids, LNPs usually include other helper lipids, such as cholesterol and poly(ethylene glycol) (PEG) lipids [60]. Cholesterol is commonly used to stabilize lipid formulations in the physiological environment [61]. Allen and Cleland found that when interacting with plasma proteins, the amount of leaked calcein in liposomes was negatively correlated with the cholesterol content, indicating that the presence of cholesterol might have tightened the phospholipid bilayers and, thus, reduced drug leakage [62]. More recently, the role of cholesterol in the subcellular transport of LNPs was emphasized. Siddharth *et al.* [63] constructed a series of cholesterol analogs and the resultant structure-activity relationship analysis showed that the incorporation of C-24 alkyl phytosterols in LNPs (eLNP) could improve the delivery efficiency of mRNA. In addition, eLNP showed higher cellular uptake and retention, which might facilitate the endosomal escape of payloads. The enhanced delivery efficiency of eLNP may be related to subcellular interactions of cholesterol derivatives, whereas further studies are required to uncover the effect of cholesterol at the subcellular level.

The significance of PEG in systemic delivery lies in its flexibility for decoration and its ability to prolong circulating time and reduce immunogenicity. After administration, LNPs might be taken up by the mononuclear phagocyte system (MPS) and be quickly cleared from the body [64]. To prolong the circulation time, Kao *et al.*, blocked MPS by pretreating the EMT6 tumor-bearing mice with a large number of blank liposomes [65]. In 1987, Allen *et al.*, proposed the concept of long-circulating liposomes and found that the insertion of monosialoganglioside (GM1) into the liposome bilayer could significantly extend the circulating half-life of liposomes [66]. In 1990, Klibanov *et al.* and Blume *et al.*, used synthetic PEG lipid derivatives to modify liposomes [67,68]. Currently, PEG decoration has been widely applied in LNP formulation by anchoring PEG derivatives, such as 1,2-

dimyristoyl-rac-glycero-3-methoxypolyethylene glycol (DMG-PEG) onto the LNP bilayer to construct long-circulating LNPs or stealth LNPs [69,70]. Doxil™ also employs a typical PEGylated LNPs, which improves the efficacy and safety of doxorubicin chemotherapy. In addition, Ryals *et al.*, used PEGylated LNPs for intravitreal delivery of mRNA and they found that LNPs containing 5% PEG showed the highest stability and delivery efficiency in the eye [71]. While a molecular understanding of how these abovementioned helper components stabilize or enhance the delivery efficacy of LNPs is generally lacking, computer simulations that could fill this gap will be discussed in a later section.

In short, the compositions of LNPs are not as complex as biological membranes, but the types and structures of lipid components, as well as their ratios, can still be highly diverse. Changes in lipid structure or lipid content ratios affect the morphology and bioactivity of the final formulation of LNPs. Therefore, the key to the rational design of LNPs lies in the development of formulations that form LNPs with specific structural and morphological properties necessary for drug delivery. Kohli *et al.*, provided a detailed introduction to the design of LNPs with an emphasis on fine-tuning LNPs' function by varying lipid structures [72]. The methodologies for LNPs design and characterization will be further discussed in the following sections.

3.1. Combinatorial Libraries and High Throughput Screening

Both the composition of lipids and the ratio of lipids to nucleic acids greatly affect the delivery efficiency of LNPs. High-throughput screening of combinatorial libraries of compounds, a common practice in medicinal chemistry, is being adopted for the screening of lipid formulations [4,73–76]. Anderson *et al.* have pioneered the use of combinatorial libraries to synthesize and evaluate lipid materials for siRNA delivery [4]. Through reactions of aliphatic amines and acrylamide or acrylates, combinatorial libraries were constructed to create a variety of lipid structures or lipid-like compounds, termed lipidoids, for either siRNA or miRNA delivery [4]. They found that the lipidoids with high delivery efficiency shared some common structures, such as amide linkages, two or more alkyl tails with a length between 8 and 12 carbons, and secondary amines. On the basis of this study, Love *et al.*, built a library of amino alcohol-based lipidoids, in which over a 100 compounds were synthesized through a ring-opening reaction between epoxides and amine substrates [74]. Through *in vitro* high-throughput screening, the leading material C12–200, consisting of a piperazine ring and five lipid tails, was identified. The C12–200 LNPs were able to formulate with five different siRNAs and simultaneously silence the target genes in mice. Later on, Dong *et al.* synthesized 103 lipopeptide or lipopolypeptide derivatives to develop a class of lipopeptide nanoparticles (LPNs) for siRNA delivery [75]. The lead material, cKK-E12, showed potent gene silencing efficiency both *in vitro* and in multiple *in vivo* models, including mice, rats, and non-human primates. Currently, an increasing number of studies are attempting to elucidate the structure-function relationship by systematically varying the lipid structural variables/factors, including chain length, degree of saturation, linker, and lipid/drug ratio [48,57,77–83]. Most recently, Zhang *et al.*, constructed a series of lipid-like compounds (FTT) by functionalizing the core structure N^1,N^3,N^5-tris(2-aminoethyl)-benzene-1,3,5-tricarboxamide derivatives (TT3) with various lipid chains [84]. In the *in vivo* study, the lead material, FTT5 LNPs, showed high delivery efficiency of mRNA encoding

human factor VIII and a base editor, respectively, to the mouse liver. Their results indicated that the chains of the lipid-like compounds are able to tune their biodegradability *in vivo*.

In addition, it is critical to explore different lipid compositions and molar ratios to optimize LNPs. To address this issue, an orthogonal experimental design has been applied to optimize the formulations of LNPs. Through the orthogonal design matrix, the factors with different levels are examined, and the optimal conditions for individual factors are then combined to obtain the lead formulation. In order to improve the delivery efficiency of lipid-like nanoparticles (LLNs) formulated with TT3, DOPE, cholesterol, and DMG-PEG2000, Li *et al.*, designed an orthogonal experiment to investigate the effect of the four components on mRNA delivery. After two rounds of orthogonal screening, formulation Hi-TT3 LLNs (TT3/DOPE/Chol/DMG-PEG2000=20/30/40/0) emerged, showing significantly higher delivery efficiency compared with the initial formulation (TT3-DSPC LLNs) [85]. To further stabilize the particle, DMG-PEG2000 was then introduced in the formulation to afford the final optimal formulation O-TT3 LLNs (TT3/DOPE/Chol/DMG-PEG2000 = 20/30/40/0.75). In another study, Hou *et al.*, also utilized an orthogonal experimental design to optimize the formulation of vitamin C lipid nanoparticles (VcLNPs) for mRNA delivery in macrophages. The optimized formulation showed seven-fold higher mRNA delivery efficiency compared with its original formulation [86].

Given the possible existence of second-order interactions between the formulation factors, lipid libraries based on the single factor analysis may not meet the optimal requirement. To overcome this limitation, Kauffman *et al.*, applied a multi-factor analysis strategy using Design of Experiment (DOE), in which serval factors, including varying lipid ratios and structures, are analyzed simultaneously [87]. They hypothesized that besides the molar ratio of the four components (ionizable lipid [C12–200], DSPC, cholesterol and lipid-anchored PEG [C14-PEG2000]), the C12–200: mRNA weight ratio, also affected the delivery efficiency of LNPs. After three rounds of screening, the optimized formulation increased the delivery potency to 7-fold higher than those previously used for siRNA delivery. Currently, multi-factor analysis using DOE has been utilized in the high-throughput screening of various LNPs, such as siRNA, mRNA, and CRISPR-Cas9 delivery systems [58,86,88,89].

4. PREPARATION OF LNPs

Currently, a variety of LNPs preparation methods have been established [1,32,90]. Commonly used conventional preparation methods include thin-film hydration method, French pressure method, ethanol/ether injection method, reverse phase evaporation method, and freeze-thawing method [6,91–95]. The characteristics of these preparation methods are summarized in Table 1. However, the traditional preparation methods of LNPs involve residual organic solvents or surfactants that may compromise the purity and safety of LNPs. In addition, wide size distribution and inconsistent encapsulation efficiency could affect scale-up production [96]. These issues motivated the modification of conventional methods and the development of novel preparation methods such as supercritical fluid reverse phase evaporation (SRPE), membrane contactor method, and active loading method [1]. Recently, microfluidic technology has also been developed in the preparation of nanoparticulate drugs [49,97–100]. In this section, we describe a few representative preparation technologies.

4.1. Supercritical Fluid Reverse-Phase Evaporation Method

Supercritical fluid (SCF) is a single-fluid substance above its critical temperature and pressure [101]. Due to its high plasticity and low toxicity, SCF was introduced as an alternative solvent in the preparation of LNPs. Commonly used SCFs include carbon dioxide (CO_2), ethanol, water, propane, and pentane. Among them, supercritical CO_2 with low critical temperature and critical pressure has been widely used in liposome preparation. SRPE is similar to the traditional reverse evaporation method, except that organic solvent is replaced by SCF. Briefly, lipids and drugs are mixed ultrasonically and dissolved in ethanol, wherein gaseous CO_2 is pumped. The temperature and pressure are maintained at a supercritical state for 30–60 min. Then, the pressure is reduced slowly to release CO_2 and a liposome dispersion is obtained. Otake *et al.*, used the SRPE method to prepare glucose liposomes [102]. The average size of the liposomes was 481 nm, and the encapsulation efficiency reached 35%. Although the consumption of organic solvent is reduced, cosolvents, such as ethanol, could influence the stability of liposomes. In 2006, Otake *et al.*, developed an improved SRPE method (ISRPE) by sealing glucose solution with lipids before introducing CO_2 [103]. Compared with liposomes prepared by SRPE and the traditional preparation methods, liposomes prepared by ISRPE had higher encapsulation efficiency, smaller particle size, and greater stability. In the same year, Otake *et al.*, used the ISRPE method to prepare chitosan-coated cationic liposomes [104]. Compared with liposomes prepared by the traditional Bangham method, the encapsulation efficiency was increased from 2% to 17%.

4.2. Membrane Contactor Method

One disadvantage of the traditional ethanol/ether injection method is that the size of the produced nanoparticles is not uniform (30–200nm) [105–107]. To solve this issue, a membrane contactor method was established by adding a membrane unit before injecting the ethanol phase into the aqueous phase in the process of ethanol injection [108–110]. Specifically, the phospholipid-containing ethanol solution is pressured into the water phase through a porous membrane. Then, the ethanol phase is contacted with a tangentially flowing aqueous phase to self-assemble into liposomes. In addition, the particle size can be adjusted by the flow rate ratio of the water phase/organic phase. For example, Jaafar-Maalej *et al.*, changed the ratio of water/organic phase flow rate from 1.6 to 2 [108]. Consequently, the particle size of the liposomes decreased from 203 nm to 61 nm, and the drug encapsulation rate was still as high as 90%. The diverse membrane materials and the controllability of the process make this method suitable for the industrial production of liposomes. At present, this method shows the potential of preparing serval hydrophobic drugs loaded liposomes, such as beclomethasone dipropionate and spironolactone [109,110]. The prepared liposomes usually have a relatively uniform particle size (100 nm) distribution and high drug encapsulation efficiency.

4.3. Microfluidic Method

To prepare LNPs encapsulating nucleic acids, early attempts used the detergent dialysis technique to encapsulate pDNA in LNPs [111]. It involves rapid mixing of hydrophobic (cationic lipids and cholesterol) and hydrophilic (pDNA) components in a detergent

containing phase. As the detergent is removed by dialysis, nanoparticles are formed simultaneously. This technique can produce small (~100 nm) stable plasmid lipid particles (SPLP) with a relatively uniform size distribution [112–115]. As ionizable lipids were introduced to LNPs formulation, an ethanol-loading approach was developed to achieve high loading efficiencies for nucleic acids (Fig. 1).

To meet the basic requirements for an *in vivo* DDS, microfluidic mixing has been generally used as an effective and controllable mixing technique [100,116]. For example, Chen *et al.*, applied a microfluidic method for rapid preparation of siRNA containing LNPs [117]. By rapid microfluidic mixing of the ethanol and water phase, a large number of LNPs were formulated. The method enabled the preparation of high-quality LNPs, which facilitated the high throughput testing of LNP-mediated siRNA delivery. Li *et al.* provided a detailed introduction to LNP preparation protocols [118]. Specifically, to encapsulate nucleic acids, such as mRNA in LNPs, the ethanol loading approach involves mixing an ethanol phase containing ionizable lipid and helper lipids (cholesterol, phospholipid, and PEG lipid) with a nucleic acid-containing aqueous phase (pH 4 citrate buffer). Subsequently, the LNPs solution is dialyzed in phosphate-buffered saline to remove the ethanol. More recently, efforts have also been devoted to microfluidic chip design. Li *et al.*, prepared a microfluidic chip with an S-shaped channel chevron structure using polydimethylsiloxane/glass [119]. Ethanol solutions of neutral and cationic lipids, siRNA buffer, and transferrin-PEG-cholesterol ethanol solutions were injected into the chip through three channels, respectively. Compared with the bulk-method (BM: Tf-PEG-Chol were introduced after mixing lipid and siRNA), the microfluidic liposomes (MF) have smaller and more uniform particle sizes (MF: 132 ± 1.6 nm, PDI = 0.129; BM: 151.8 ± 1.8 nm, PDI = 0.216) and higher gene silencing efficiency (MF: 81% > BM: 69%). Moreover, microfluidic liposomes exhibited better antitumor effect (MF: 60.4% > BM: 14%). These results demonstrated that microfluidic technology could be used to prepare LNPs with a more uniform particle size and improved biological effects. In order to improve the production scale of microfluidic technology, Hood *et al.*, designed a microfluidic vertical flow focusing (VFF) device with a high aspect ratio (depth: width =100:1) [120]. This high aspect ratio system greatly enhanced the production rate of liposomes. The size of prepared liposomes is 80–200 nm and the production rate reached 1.6 mg/min (100 mg/h). Currently, the ethanol loading technique combined with microfluidics is a generally applicable process for efficient encapsulation of siRNA, mRNA, pDNA, as well as other negatively charged entities.

4.4. Active Loading Method

The conventional passive loading method does not contain a specific drug-loading step [121]. Drugs are dissolved in the aqueous phase or organic phase (based on their solubility) and drug loading occurs during the process of preparation. Thus, the passive loading method is not suitable for amphiphilic drugs because their oil-water partition coefficient is greatly affected by the pH and ionic strength of the medium. In contrast, the active loading method utilizes the gradients of ions or compounds across the liposome membrane as the driving force to encapsulate drugs. Commonly used active drug loading methods include pH gradient method [8,122], ammonium ion gradient method [123], and ionophore-mediated ion gradient method [124]. The pH gradient method is a more classic method and generally

used for loading of weakly basic drugs. Doxil™ is a representative example of the pH gradient method. In the preparation of Doxil™, a pH gradient is created when the external phase of liposomes is exchanged with Na_2CO_3. As doxorubicin is a weak base, it is in equilibrium between ionization and molecularization. The non-ionized state of doxorubicin can pass through the lipid bilayer and be ionized and trapped inside the vesicles [125]. Basically, drugs, such as doxorubcin, are easy to be incorporated into liposomes and have excellent retention properties, while non-weak base drugs, such as paclitaxel, can be converted into weak base prodrugs to facilitate encapsulation [126].

5. CHARACTERIZATION OF LNPs IN EXPERIMENTS

5.1. Size and Zeta Potential

The function of LNPs is closely related to their structural and physical properties [127]. Measurement and analysis of LNP parameters, such as particle size, concentration, and zeta potential can help screen the LNP formulation or predict the effectiveness of the LNPs in bioassays. Fig. (2) summarizes representative methods for LNPs characterizations. The size of a nanoparticle is an important parameter that can be tailored to control particle distributions *in vivo* [128]. Dynamic light scattering (DLS) and tracking analysis technology (NTA) are widely used technologies for measuring particle size [129,130]. The principle of the DLS is based on the Stokes-Einstein equation; that is, when spherical particles obey the Brownian motion law in a dilute solution, the intensity of the scattered light is proportional to the sixth power of the particle diameter. Because the influence of large particles on the scattered light intensity is much greater than that of small particles, the DLS is suitable for systems with a un form particle size distribution and can sensitively reveal particle aggregation. The principle of the NTA is similar to the DLS, but NTA has a higher resolution and the measurement results are not significantly affected by the sample concentration. NTA combines light scattering microscopy and video imaging technology to measure the particle size in the range of 10–2000 nm. The NTA technology can also perform separate analysis and track individual particles; therefore, the detected particles can be clearly distinguished and the measurement of the relative light scattering intensity of individual LNPs can be obtained. Similar to particle size measurement, the zeta potential of LNPs helps to predict their pharmacokinetic characteristics in the body [131]. The zeta potential has also been used to optimize the ratio of specific LNPs to different pDNA, thereby minimizing the degree of aggregation of the formulation [132]. The technique of laser Doppler velocimetry is widely used for determining the zeta potential of LNPs. The technology applies an electric field to the particle dispersion to drive the motion of particles and the zeta potential can be calculated based on the electrophoretic mobility [133,134]. It is worth noting that the zeta potential is highly sensitive to the environment, such as pH or ionic strength. Therefore, the measurement of the diluted solution may not be able to reflect the actual zeta potential of the concentrated suspension [135].

5.2. Morphology

Atomic Force Microscope (AFM), cyro-TEM, and X-ray scattering are the general methods for morphologic characterization of nanoparticles [136]. In recent years, high-resolution cryo-TEM has played an increasingly important role in the study of the morphology and

structure of nanoparticles, including liposomes and other LNPs [137]. For example, Doxil™ and Myocet™ are two commercially available doxorubicin liposome formulations. Their aqueous phases contain two nanocrystals of doxorubicin-sulfate and doxorubicin-citrate, respectively, both of which are bundle structures made of fiber. According to the results measured by cryo-TEM and X-ray scattering, the average distance between the fibers in doxorubicin-citrate crystal bundles (3.0 to 3.5 nm) is larger than that in doxorubicin-sulfate crystal bundles (2.7 nm), which might be explained by the larger volume of citrate ions than sulfate ions [138,139]. More recently, structures of LNPs for nucleic acid delivery have also been characterized by the cryo-TEM and small-angle X-ray scattering methods that not only visualized LNPs but also studied the mechanism of nanoparticle formation [136]. For example, by observing the electron-dense structure using the cryo-TEM and small-angle X-ray scattering methods, Kulkarni *et al.* [136] found that LNP-siRNA showed a small multilayer structure at high siRNA content, in which nucleic acids were located between tightly bound bilayers. At low siRNA content, the LNP-siRNA system exhibited a combined structure consisting of siRNA double-layers and amorphous electron-dense core. Using the X-ray scattering methods, some recent studies re-examined the structure of LNPs and showed that the electron dense core morphology of LNPs is not composed of reverse micelles, but an oil core of neutral ionizable lipids, which implies that the LNP-siRNA is formed by the fusion of smaller particles after the rapid mixing process [98]. Morphological studies may help to understand the structure of LNPs but also hold limitations because the original structures (especially the composite structures) could be interfered during the assessment. For instance, in AFM, the sample is usually placed on the surface of the mica, which may interact with the lipid components and the original structure of the nucleic acid complex. Therefore, multiple characterization techniques should be applied to improve the accuracy of structural analysis.

5.3. *In Vitro* Evaluation of LNPs

Cell studies may help characterize the functions of LNPs, including cytotoxicity, endocytosis mechanism, and delivery activity. Based on the LNPs and therapeutic purpose, specific cell experiments can be designed to provide the details at the cellular or subcellular level. For example, to investigate the mechanism of siRNA LNPs' entry into liver cells, Gilleron *et al.*, used quantitative fluorescence imaging and electron microscopy to monitor the uptake profile of siRNA LNPs in HeLa cells. They found that LNPs enter cells through clathrin-mediated endocytosis and micropinocytosis. Further, they estimated that only 1–2% of siRNA could escape from the endosome into the cytosol after endocytosis [140].

In the past decades, researchers have developed many reporter genes as model payloads to characterize the delivery efficiency of LNPs [56,141–147]. Basically, an ideal reporter gene does not exist in the cell model or can be easily distinguished from its natural form. In addition, it should be convenient for measurement and has a wide linear detection range. Commonly used reporter genes include plasmids encoding luciferase, nuclear-targeted β-galactosidase, secreted alkaline phosphatase (SEAP), green fluorescent protein (GFP), and chloramphenicol transferase [148]. In addition to serving as model genes, the reporter gene can also be used as control for standardizing delivery efficiency. For example, a HeLa cell line that simultaneously expresses firefly (*Photinus pyralis*) and *Renilla* (*Renilla reniformis*)

luciferase were used to characterize the lipidoid-mediated delivery of siRNA [4]. In this study, siRNA targeted firefly luciferase and *Renilla* luciferase served as a control. The siRNA delivery efficiency was determined by the ratio between a firefly and *Renilla* luciferase expression after treating the cells with lipidoid-based LNPs. In another study, Ball *et al.*, used the firefly luciferase gene targeting siRNA and the fluorescent protein mCherry encoding mRNA to investigate the co-delivery efficiency of the LNPs [82]. By quantifying the fluorescence intensity of the luciferase and the mCherry, both translation of mRNA and gene silencing of siRNA were characterized.

Due to the difference between *in vitro* and *in vivo* conditions, the *in vitro* results may not well predict *in vivo* delivery [69,149]. Recently, researchers are directly conducting *in vivo* screening based on the therapeutic purpose [150–154]. For example, Dahlman *et al.*, reported DNA barcoded nanoparticles, which realized *in vivo* high-throughput screening of hundreds of different nanoparticles with interesting chemical structures [153]. A large volume of animal results was obtained by the combination of high throughput chemistry, high throughput nanoparticle formulation, and next-generation DNA sequencing [150–152]. Similarly, Guimaraes *et al.*, developed a barcoded mRNA library by modifying mRNA with a barcoded region [154]. Different mRNA incorporated LNPs were pooled and administered intravenously into mice. The functional delivery of mRNA can be quantified using deep sequencing for the screening of lead formulations.

6. COMPUTATIONAL APPROACHES FOR STUDIES OF LNPs

Computational studies, especially multiscale modeling and simulations, bridge the gap between molecular mechanisms and experimentally measured properties of LNPs-based DDS across multiple length and time scales (Fig. 3). In the following sections, we will focus on the multiscale computational modeling of LNPs using molecular dynamics (MD) simulation.

In general, computer simulation consists of two parts: the physical representation of the system of interest and the algorithms used to simulate the dynamic behavior of the system or to generate a conformational ensemble of the system. An MD simulation generates a movie of a set of particles giggling over time using the Newtonian equation of motion from which the average structural and physical properties of the system can be derived using statistical mechanics [155]. Sufficient conformational sampling is warranted to obtain statistically meaningful thermodynamic and structural properties. MD simulation has been widely used to study biological and soft matter systems.

Multiscale computational approaches involve a physical description of the systems with multiple levels of details. At the highest level of details, a molecular system is described using quantum mechanics (QM). QM calculations have been widely applied either directly to systems, such as carbon nanotubes, quantum dots, and magnetic nanoparticles, or indirectly to the derivation of models for less detailed simulations (e.g. MD simulations). In practice, however, QM calculations are limited to small systems with limited degrees of freedom. If only part of the system requires QM treatment, one can resort to hybrid QM and molecular mechanical (MM) models, namely QM/MM [156–158].

To simulate larger systems, one can simplify the systems by averaging out the electron degrees of freedom and representing them as partial charges on atoms. Under the framework of MM, atoms are described as van der Waals (vdW) spheres with charges that interact through empirical electrostatic and Lennard-Jones (LJ) forces. The notion of molecules is introduced by holding all atoms together using harmonic restraint potentials, such as bond, angle, and dihedral terms. One limitation of MM is that atoms are described as point charges, meaning that some important electronic effects like polarization, charge transfer, or π-electron clouds are ignored. Such a limitation can be overcome by the abovementioned QM/MM calculations. The set of interaction parameters in MM is called a force-field, which is generally built from QM calculations and experimental data. Examples of commonly used force-fields include AMBER (current version: 14 [159]), CHARMM (current version: 36m for amino acids [160], 36 for lipids [161] and 36 for DNA [162] and RNA [163]), and OPLS-AA [164]. Among them, CHARMM force-fields have drawn the most usage for MD simulations involving lipids. Accuracy and reproducibility of the force-fields have been reviewed elsewhere for interested readers [165,166]. Over the decades, MD has been developed into a mature technique implemented in a number of software packages, including CHARMM [167], AMBER [168], NAMD [169], GROMACS [170], OpenMM [171], and LAMMPS [172]. A typical result of an MD simulation is a trajectory (or a movie) of all atoms in the system with the spatial and temporal scales limited to $10–10^2$ nanometers (nm) and 0.1–10 microseconds (μs) with contemporary computing resources. In practice, through coarse graining, the length and time scales of MD simulations can be extended by one (sometimes even two) order(s) of magnitude to accommodate the need of simulating nanoparticles of size >100 nm.

Coarse graining in MD simulations often refers to building models in which particles do not represent atoms, but rather groups of atoms. A typical coarse graining scheme involves two parts: first is the grouping of atoms to form coarse-grained (CG) beads, and second is the parameterization of effective potential (or interactions) for the CG beads. Two general approaches have been extensively explored for MD simulations of chemical or biomolecular systems. One is the chemistry-based approach represented by the MARTINI model [173]; the other is the physics-based approach [174]. In MARTINI models, lipids are represented by head group beads and each with two or more tail beads to reproduce some generic properties of the molecules. Based on the chemical nature of the underlying structure, the CG beads are assigned specific particle types with varying polarity. The interaction between the beads is described by a simple and empirical LJ potential with a strength depending on the interacting bead types. In contrast, a physics-based coarse graining scheme creates beads from identifying atoms of similar dynamics and parameterizes them through force-matching [175,176] or reproducing atomic fluctuations [177]. The force-matching method has made promising progress in simulating multicomponent lipid bilayers in its early stage of development [178–180], which has provided valuable insights into protein self-assembly [181] but has been less commonly used for LNPs simulations compared to the MARTINI models. We note that these two approaches are incompatible with each other, meaning that combining CG beads constructed using one approach with effective interactions parameterized using the other approach would lead to incorrect simulations.

Coarse graining schemes have stretched the limits of MD simulations towards hundreds of nanometers (nm) and microseconds (μs). In order to explore the even greater length and time scales, one has to replace the dynamics propagation scheme in MD with other algorithms, such as Brownian dynamics (BD) [182,183], Langevin dynamics (LD) [184], or dissipative particle dynamics (DPD) [184,185]. Furthermore, solvent-free phase field-based methods in which a system is described by density or friction fields have been used to study extremely large-scale biomembranes, i.e., vesicle mimicking a red blood cell, using anisotropic stochastic dynamics with hydrodynamic interactions [186]. Such membrane dynamics in the fluid environments derived from first principles can be coupled with the abovementioned coarse-graining schemes, therefore, further boosting the scope of molecular simulations. Recent examples include simulating vesicle fission and membrane bud formation by combining the MARTINI model with a dynamical triangulated surface (DTS) on which slow large-scale membrane conformational changes were quickly sampled [187]. Although DTS and similar approaches were successful in describing the shape of simple membranes [188–191], only with the development of back-mapping from a mesoscopic model to a CG or atomistic model [187] could the important molecular details be revealed through these multiscale simulations.

7. MOLECULAR SIMULATIONS OF LNPs AND RELATED SYSTEMS

7.1. Simulation of Lipid Bilayers

As mentioned in an earlier section, in addition to lipids, LNPs often contain other molecular components, such as sterols, carotenoids, fat-soluble vitamins, and even cargos they carry. To rationally design and optimize an LNP-based DDS, a molecular-level understanding of how small molecules interact with lipid membranes is crucial. These interactions govern the assembly and distribution of small molecules in terms of their transversal location and orientation and lateral partitioning in the membranes. Vice versa, the same interactions also control how lipid bilayers may be influenced by the presence of small molecules, including membrane structure (ordering, packing, curvature), membrane electrostatic potentials, membrane mechanical properties (lateral pressures, rigidity), and membrane permeability, which may, in turn, affect small molecules' partitioning in the membranes and determine the drug-carrying ability of specific LNPs. Membrane-small molecule interactions are truly a mutual effect between membranes and small molecules. The chemical and structural properties of small molecules cannot solely account for their interactions with (partition in) the membranes. The composition, structural, and phase properties of the membranes also play important roles in shaping their interactions with (accommodation of) small molecules. Many molecules, such as sterols [192–194], carotenoids [195,196], or vitamins [197,198], have been reported to partition into membranes and, in turn, affect membrane structures and properties. Readers are referred to a recent comprehensive review on how membrane organization can be modulated by specific membrane components and, in turn, shape the membrane's cellular function [199].

An important quantity for characterizing small moleculelipid interactions is permeability - the ability of a drug molecule passing through the membranes - which usually involves the determination of molecular diffusivity and partitioning. While the experimental

measurement of the overall permeability is possible, molecular details of the permeation process have mainly come from computational studies. In general, experiments only allow the measurement of the overall permeability coefficient and are unable to separate the contributions from diffusion and partitioning. In addition, the dynamic diffusion processes are very difficult to probe by experiments. Computer simulations are ideally suited for the investigation of both partitioning and diffusion of small molecules in lipid bilayers. To reduce the computational cost, atomistic simulations of lipid bilayer patches have been commonly employed to infer results on partitioning and diffusion of small molecules in liposomes [200,201] (Fig. 4A).

Early MD studies of the membrane permeation processes were carried out by Marrink and Berendsen [202,203]. By constraining a small molecule at a given position inside a lipid bilayer, both diffusion coefficients and partitioning free energies were calculated through the analyses of the positional fluctuations and the forces required to maintain the position constraints. Comparison of simulation results with limited experimental data has shown that membrane permeability depends on multiple factors [203–208]. Generally, hydrophilic molecules come across a free energy barrier when entering the hydrocarbon core of the membrane, whereas hydrophobic molecules tend to reside in the hydrocarbon region of the membrane [205]. There is, in general, a good correlation between a molecule's free energy in the center of the membrane (relative to the bulk water) with its experimental partition results between water and hexadecane. Interestingly, Bemporad *et al.*, reported that the size of small molecules has a more pronounced effect on their partitioning than their diffusion in lipid bilayers [204]. One example is benzene, which interferes with the lateral packing of lipid tails due to its relatively large size, but shows little difference in its diffusional behavior compared to other smaller molecules. Later, Comer and Chipot [207,208] suggested a sub-diffusive model in which a position-dependent fractional-order quantifies how the motion of the molecule deviates from classical diffusion along the membrane's normal direction. By studying a homolog series of short-tail alcohols, they first showed that the free-energy barriers for passage through the center of the bilayer decrease with the length of the aliphatic alcohol chains, in quantitative agreement with experimentally determined differential solvation free energies in water and oil. Then they employed the sub-diffusive model to show that a molecule's permeability is predominantly determined by such free-energy differences, whereas the fractional diffusivity near the center of the membrane is similar among the molecules despite the large difference in their molecular weight and lipophilicity. The strategy was further developed into more affordable membrane permeability calculations [209] in which one can compute the free-energy profile with a series of free-energy perturbation calculations and the diffusivity profile with a series of adaptive biasing force calculations using a Bayesian-interference scheme [210,211]. For a detailed discussion of small molecules permeating across biological membranes, readers are referred to more focused reviews [212,213].

7.2. Simulation of PEGylated Membranes

PEGylation has been successfully used to increase the circulation time of drug delivery liposomes by forming a protective PEG layer over the liposomal surface so as to provide an external steric sheath. It was reported that this layer prevents the interaction with opsonins,

thus reducing the drug uptake by immune cells [67]. However, how PEGylated lipids interact with various surrounding molecules, such as other lipids and solvent molecules, to shape their localization and steric effect is unclear.

MD simulations have been particularly useful in providing a mechanistic understanding of how PEGylation improves the drug-loading efficiency of membranes. Dzieciuch *et al.*, for instance, performed atomistic MD simulations to study how a hydrophobic molecule, 5,10,15,20-tetrakis(4-hydroxyphenyl)porphyrin (p-THPP), interacts with lipid bilayers [214]. In agreement with experiments, p-THPP enters both zwitterionic and PEGylated membranes. While the free volume of p-THPP decided its localization in the zwitterionic membranes, i.e., in the PEGylated membranes, the p-THPP could wrap with the PEG corona. Therefore, p-THPP showed greater solvent exposure in PEGylated liposomes than in zwitterionic ones. Similar MD simulations have been utilized to explain the failure in improving the targeting of activated endothelium targeting peptide (AETP) using PEGylated liposomes [215]. The simulations revealed that the bonded AETP moiety was located within the PEG layer and is, thus, less exposed than other more hydrophilic peptides. It has also been shown that, under physiological conditions, PEG tends to coil around the ions, which increases the exposure of the nonpolar ethylene groups and, thus, the effective hydrophobicity of the molecule. Such increased exposure granted a protective role to PEG molecules for drug molecules, such as hematoporphyrin [216]. A PEGylated micelle has also been studied with similar approaches [217,218]. Vukovic *et al.*, [218] showed that hydrophobic molecules, such as bexarotene, can reside both in the alkane core center by assembling into a cluster and at the micellar ionic interface of the PEG corona with their polar ends pointing out to the solvent. By contrast, hydrophilic molecules, such as a human vasoactive intestinal peptide, are mostly stabilized at the ionic interface by electrostatic interactions between their positively charged residues and the negatively charged head-groups of the lipids.

The interactions of PEG with various other essential LNP components, such as cholesterol [193,219–221] or ions [222,223], have also been investigated by MD simulations. Magarkar *et al.*, [219] have shown through atomistic MD simulations that PEG enters the lipid bilayer in a specific fashion by aligning with the β face of the cholesterol molecule. Additionally, PEG interferes with the role of cholesterol in structuring and compacting the membrane; when the membrane is PEGylated, the area per lipid increases, rather than decreasing, with increasing cholesterol. The surface charge of LNPs is crucial to their delivery behavior. Magarkar *et al.*, [222] used atomistic MD simulations to show that increasing the PEGylated lipid concentration caused the PEG layer to become effectively positively charged and, thus weaken its interaction with cations, providing an atomic-level explanation for the inhibition of calcium-induced liposome fusion by PEGylation observed experimentally.

Tremendous technical advances have been made in liposome-based drug delivery over the past decades, leading to numerous clinical trials in delivering a diverse variety of drugs. By inferring information from atomistic simulations of lipid bilayers, one could not only provide mechanistic explanations for experimental observations but also make predictions on the effects of specific chemical modifications or re-formulations. Readers are referred for

more specific reviews on PEGylated LNPs [224–226] and other ligand-conjugated LNPs [227].

7.3. Simulation of Liposomes and Micelles

Although useful in providing rich information on the structure and dynamics of lipid bilayers at the molecular level, all-atom MD simulations are unable to probe large-scale structures and dynamics of liposomes, such as morphological properties, undulation dynamics and self-assembly processes, which could be critically related to the systems' delivery efficiency. Therefore, researchers have attempted to interrogate lipid-based DDS with a simulation at coarser resolutions (Fig. 4B). Coarse-graining preserves most of the structural and chemical properties of individual molecules in liposomes [228] while providing the opportunity to probe their biologically relevant dynamics, such as vesicle formation [229–235], fission, and fusion [236–241].

The MARTINI CG model has been widely applied to construct liposomes or micelles of various sizes. With the availability of such models, the physical stability of lipid nanoparticles could be evaluated [242–244]. By studying highly curved liposomal membranes (diameter of 15–20 nm) using CGMD simulations, Risselada and Marrink [245] revealed a general packing effect in which closely packed lipid heads and disordered lipid tails were found in the inner monolayer, whereas the opposite was seen in the outer monolayer. By mixing PC and phosphatidylethanolamine (PE) lipids, a clear tendency toward partial transversal demixing of the two components, especially with PE lipids enriched in the inner monolayer, was observed. This observation is in line with the static shape concepts that inverted-cone-shaped lipids, such as PE, would prefer the concave volume of the inner monolayer and has been used to rationally design cationic lipids for siRNA delivery [246]. Interestingly, molecular simulations also revealed that the ability of the polyunsaturated lipid tails to backfold could also drive invertedcone-shaped lipids towards the outer monolayer.

CG simulations have also been carried out to assess the performance of liposomes as drug carriers [247–250]. For instance, hypericin, an efficient photosensitizer for photodynamic therapy, was found close to the polar headgroup region of the outer lipid layer and orient so as to maximize the interactions with the lipid interior using its more hydrophobic end [247]. CGMD simulations also revealed that siRNA duplexes were complexed with cationic lipids and clustered in the interior core of the LNPs, together with phospholipids and cholesterols [251]. On the other hand, Menichetti *et al.* performed high-throughput CGMD simulations to screen 119 molecules and identified the key features of the effective partitioning free energy profiles that correlate with experimentally determined partitioning coefficients [252]. Furthermore, they revisited the Meyer-Overton rule for drug-membrane permeability and found that the permeability coefficient of a compound is determined by its partitioning free-energy and pKa constant [253]. The established correlation between specific chemical groups and the resulting permeability coefficients enabled an inverse design strategy and suggested that the predominance of commonly employed chemical moieties might have unintentionally limited the range of permeability [254].

On larger length and time scales, DPD [255–259] and continuum models [260] have been used to study the behavior of lipid vesicles in fluid flow. The early approaches included BD simulations [182,183,261,262], by which Noguchi *et al.*, studied the fusion dynamics of vesicles that are highly relevant to the cell uptake of lipid-based DDS [262].

Molecular simulations can impact the novel DDS development both directly and indirectly. While capable of directly predicting the stability and morphology of LNPs, CGMD simulations are more often employed to provide mechanistic insights into the membrane systems of interest, such as structural properties, lipid-small molecule interactions, which can, in turn, be used to guide LNP composition optimization or chemical modification for better delivery efficiency.

8. FORMULATION DESIGN AND OPTIMIZATION FOR LNPs

A typical approach to formulate LNPs is to establish a quantitative structure-activity relationship (QSAR) between their compositions and *in vitro*/*in vivo* activities. Nevertheless, such phenomenological models with layers of unknown factors are still facing significant challenges in the optimization of even well-established formula. Furthermore, a missing link between *in vitro* and *in vivo* behaviors of LNPs has raised the concern of establishing clinically relevant QSAR models. As a result, tremendous efforts have been devoted to searching for one or more intermediate points in-between the formula of an LNP and its clinical behaviors [263]. For example, the phase behavior of LNP systems, which may serve as a bridge between LNP formulation and *in vitro* or *in vivo* delivery performance, with varying ratios of saturated and unsaturated fatty acids [264] or lipids with different chain lengths [265,266], has been successfully predicted using machine learning. Other examples include predicting antibacterial profiles [267] or toxicity [268,269] from LNPs formulations. Gonzalez-Diaz *et al.* [270] reported a general perturbation approach for building QSAR models. They derived and validated several non-classical QSAR-perturbation models and used them to predict a wide range of properties, from assessment of ADME (absorption, distribution, metabolism, excretion) properties of chemicals to the rational selection of the components of cancer co-therapy drug-vitamin release nanoparticles [271] or coated nanoparticles [272]. Yamankurt *et al.*, quantitatively modeled spherical nucleic acid (SNA) immune activation and identified the minimum number of SNAs needed to build an optimal QSAR for a given SNA library [273]. Readers are referred to more specific reviews on how to accurately predict biomedically relevant properties of nanoparticles from experimental and computational data [274,275].

Another method to enhance the predictive power of QSAR models of LNP formulations is to bridge experimental measurements with information obtained from molecular simulations. Metwally *et al.* [276] demonstrated a computer-assisted drug formulation design process for estimating the loading of different drugs on their potential carriers. They utilized several structural modeling and informatics tools, such as MD simulations, molecular docking, data mining, and artificial neural networks. First, MD simulations were used to simulate the nanoparticles with specific formulation or compositions. Then, binding free energies of drugs to their potential nanoparticle carriers were obtained through molecular docking calculations. Together with the experimental data gathered from the literature, an artificial

neural network was built to correlate the features of the formulation to the experimental and computational loading efficiency data. A similar approach was extended to solid lipid nanoparticles [277] and microemulsions [278].

CONCLUSION AND PERSPECTIVES

Studies on lipid nanoparticle-based drug/gene delivery systems cover a wide range of spatial resolutions, and require multiple disciplines of physics, chemistry, and biotechnology to be integrated. Formulation and preparation of LNPs necessitate training in chemistry, and characterization of LNPs using various spectroscopic and microscopic measurements entails knowledge in biophysics or soft matter physics. To understand the dynamics of LNPs at the atomic level, computer simulations are often needed to bridge LNPs' molecular structures with their biological activities. Yet, the clinically relevant efficiency and robustness of the DDS of interest are still extremely difficult to predict, even from *in vivo* results. As an example, only a small number of nucleic acid-based therapeutics have been approved for clinical use. This obviously reflects the challenges inherent in the development of LNPs.

Therefore, to accelerate the development of DDS, there is an urgent need for integrated studies that combine computational and experimental approaches. Two common themes in the integrated studies of LNPs have been reviewed. First, studies have been carried out to establish relationships between the structural and the functional properties of nanoparticles. Second, efforts have been made to optimize the formulation of nanoparticles by either directly predicting their functional performance or predicting their structural properties that can then be related to the functional performance. We believe that integrating molecular simulations into these studies could bridge the two existing themes and, thus fill a critical gap between LNPs' formulation and their biological activities. As an example, in a previous study [264], phase behavior (functional performance) of a nanoparticle was correlated with the particle size (structural property) or lipid chain length (molecular feature), while the effects of lipid chain length on particle size could be revealed through CGMD simulations [279]. We envision that unlocking next-generation formulation of LNPs delivery systems will necessitate taking full advantage of massive experimental and computational data to elucidate the fundamental principles underlying the drug/gene delivery processes.

FUNDING

Y.D. acknowledges the support of the Maximizing Investigators' Research Award R35GM119679 from the National Institute of General Medical Sciences, as well as the start-up fund from the College of Pharmacy at The Ohio State University. X.C. acknowledges the start-up fund from the College of Pharmacy at The Ohio State University.

REFERENCES

[1]. Pattni BS; Chupin VV; Torchilin VP New Developments in Liposomal Drug Delivery. Chem. Rev, 2015, 115(19), 10938–10966. 10.1021/acs.chemrev.5b00046 [PubMed: 26010257]

[2]. Allen TM; Cullis PR Liposomal drug delivery systems: from concept to clinical applications. Adv. Drug Deliv. Rev, 2013, 65(1), 36–48. 10.1016/j.addr.2012.09.037 [PubMed: 23036225]

[3]. Akinc A; Maier MA; Manoharan M; Fitzgerald K; Jayaraman M; Barros S; Ansell S; Du X; Hope MJ; Madden TD; Mui BL; Semple SC; Tam YK; Ciufolini M; Witzigmann D; Kulkarni JA; van der Meel R; Cullis PR The Onpattro story and the clinical translation of nanomedicines

containing nucleic acid-based drugs. Nat. Nanotechnol, 2019, 14(12), 1084–1087. 10.1038/s41565-019-0591-y [PubMed: 31802031]

[4]. Akinc A; Zumbuehl A; Goldberg M; Leshchiner ES; Busini V; Hossain N; Bacallado SA; Nguyen DN; Fuller J; Alvarez R; Borodovsky A; Borland T; Constien R; de Fougerolles A; Dorkin JR; Narayanannair Jayaprakash K; Jayaraman M; John M; Koteliansky V; Manoharan M; Nechev L; Qin J; Racie T; Raitcheva D; Rajeev KG; Sah DWY; Soutschek J; Toudjarska I; Vornlocher H-P; Zimmermann TS; Langer R; Anderson DG A combinatorial library of lipid-like materials for delivery of RNAi therapeutics. Nat. Biotechnol, 2008, 26(5), 561–569. 10.1038/nbt1402 [PubMed: 18438401]

[5]. Bangham AD; Horne RW Negative Staining of Phospholipids and Their Structural Modification by Surface-Active Agents as Observed in the Electron Microscope. J. Mol. Biol, 1964, 8, 660–668. 10.1016/S0022-2836(64)80115-7 [PubMed: 14187392]

[6]. Bangham AD; Standish MM; Watkins JC Diffusion of univalent ions across the lamellae of swollen phospholipids. J. Mol. Biol, 1965, 13(1), 238–252. 10.1016/S0022-2836(65)80093-6 [PubMed: 5859039]

[7]. Sessa G; Weissmann G Phospholipid spherules (liposomes) as a model for biological membranes. J. Lipid Res, 1968, 9(3), 310–318. [PubMed: 5646182]

[8]. Butu A; Rodino S; Golea D; Butu M; Butnariu M; Negoescu C; Dinu-Pirvu C-E Liposomal Nanodelivery System for Proteasome Inhibitor Anticancer Drug Bortezomib. Farmacia, 2015, 63, 224–229.

[9]. Xu X; Saw PE; Tao W; Li Y; Ji X; Bhasin S; Liu Y; Ayyash D; Rasmussen J; Huo M; Shi J; Farokhzad OC ROS-Responsive Polyprodrug Nanoparticles for Triggered Drug Delivery and Effective Cancer Therapy. Adv. Mater, 2017, 29(33)1700141 10.1002/adma.201700141

[10]. Lin Y-X; Wang Y; An H-W; Qi B; Wang J; Wang L; Shi J; Mei L; Wang H Peptide-Based Autophagic Gene and Cisplatin Co-delivery Systems Enable Improved Chemotherapy Resistance. Nano Lett, 2019, 19(5), 2968–2978. 10.1021/acs.nanolett.9b00083 [PubMed: 30924343]

[11]. Shi J; Xiao Z; Votruba AR; Vilos C; Farokhzad OC Differentially charged hollow core/shell lipid-polymer-lipid hybrid nanoparticles for small interfering RNA delivery. Angew. Chem. Int. Ed. Engl, 2011, 50(31), 7027–7031. 10.1002/anie.201101554 [PubMed: 21698724]

[12]. Xue Y; Feng J; Liu Y; Che J; Bai G; Dong X; Wu F; Jin T A Synthetic Carrier of Nucleic Acids Structured as a Neutral Phospholipid Envelope Tightly Assembled on Polyplex Surface. Adv. Healthc. Mater, 2020, 9(6)e1901705 10.1002/adhm.201901705 [PubMed: 31977157]

[13]. Russick J; Delignat S; Milanov P; Christophe O; Boros G; Denis CV; Lenting PJ; Kaveri SV; Lacroix-Demazes S Correction of Bleeding in Experimental Severe Hemophilia A by Systemic Delivery of Factor VIII-Encoding MRNA. haematologica, 2020, 105, 11129–1137.

[14]. James ND; Coker RJ; Tomlinson D; Harris JRW; Gompels M; Pinching AJ; Stewart JSW Liposomal doxorubicin (Doxil): an effective new treatment for Kaposi's sarcoma in AIDS. Clin. Oncol. (R. Coll. Radiol.), 1994, 6(5), 294–296 10.1016/S0936-6555(05)80269-9 [PubMed: 7530036]

[15]. Barenholz Y Doxil®--the first FDA-approved nano-drug: lessons learned. J. Control. Release, 2012, 160(2), 117–134. 10.1016/j.jconrel.2012.03.020 [PubMed: 22484195]

[16]. Beltrán-Gracia E; López-Camacho A; Higuera-Ciapara I; Velázquez-Fernández JB; Vallejo-Cardona AA Nanomedicine Review: Clinical Developments in Liposomal Applications. Cancer Nano, 2019, 10, 11. 10.1186/s12645-019-0055-y

[17]. Maurer N; Fenske DB; Cullis PR Developments in liposomal drug delivery systems. Expert Opin. Biol. Ther, 2001, 1(6), 923–947. 10.1517/14712598.1.6.923 [PubMed: 11728226]

[18]. Park H-J; Yang F; Cho S-W Nonviral delivery of genetic medicine for therapeutic angiogenesis. Adv. Drug Deliv. Rev, 2012, 64(1), 40–52. 10.1016/j.addr.2011.09.005 [PubMed: 21971337]

[19]. Cullis PR; Hope MJ Lipid Nanoparticle Systems for Enabling Gene Therapies. Mol. Ther, 2017, 25(7), 1467–1475. 10.1016/j.ymthe.2017.03.013 [PubMed: 28412170]

[20]. Mukalel AJ; Riley RS; Zhang R; Mitchell MJ Nanoparticles for nucleic acid delivery: Applications in cancer immunotherapy. Cancer Lett, 2019, 458, 102–112. 10.1016/j.canlet.2019.04.040 [PubMed: 31100411]

[21]. Veiga N; Diesendruck Y; Peer D Targeted lipid nanoparticles for RNA therapeutics and immunomodulation in leukocytes. Adv. Drug Deliv. Rev, 2020. S0169–409X(20)30022–3

[22]. Hoffman RM; Margolis LB; Bergelson LD Binding and entrapment of high molecular weight DNA by lecithin liposomes. FEBS Lett, 1978, 93(2), 365–368. 10.1016/0014-5793(78)81141-7 [PubMed: 568565]

[23]. Mannino RJ; Allebach ES; Strohl WA Encapsulation of high molecular weight DNA in large unilamellar phospholipid vesicles. Dependence on the size of the DNA. FEBS Lett, 1979, 101(2), 229–232. 10.1016/0014-5793(79)81014-5 [PubMed: 446747]

[24]. Dimitriadis GJ Entrapment of ribonucleic acids in liposomes. FEBS Lett, 1978, 86(2), 289–293. 10.1016/0014-5793(78)80582-1 [PubMed: 624413]

[25]. Fraley R; Straubinger RM; Rule G; Springer EL; Papahadjopoulos D Liposome-mediated delivery of deoxyribonucleic acid to cells: enhanced efficiency of delivery related to lipid composition and incubation conditions. Biochemistry, 1981, 20(24), 6978–6987. 10.1021/bi00527a031 [PubMed: 6274382]

[26]. Fraley R; Subramani S; Berg P; Papahadjopoulos D Introduction of liposome-encapsulated SV40 DNA into cells. J. Biol. Chem, 1980, 255(21), 10431–10435. [PubMed: 6253474]

[27]. Felgner PL; Gadek TR; Holm M; Roman R; Chan HW; Wenz M; Northrop JP; Ringold GM; Danielsen M Lipofection: a highly efficient, lipid-mediated DNA-transfection procedure. Proc. Natl. Acad. Sci. USA, 1987, 84(21), 7413–7417. 10.1073/pnas.84.21.7413 [PubMed: 2823261]

[28]. Vangasseri DP; Cui Z; Chen W; Hokey DA; Falo LD Jr; Huang L Immunostimulation of dendritic cells by cationic liposomes. Mol. Membr. Biol, 2006, 23(5), 385–395. 10.1080/09687860600790537 [PubMed: 17060156]

[29]. Filion MC; Phillips NC Toxicity and immunomodulatory activity of liposomal vectors formulated with cationic lipids toward immune effector cells. Biochim. Biophys. Acta, 1997, 1329(2), 345–356. 10.1016/S0005-2736(97)00126-0 [PubMed: 9371426]

[30]. Semple SC; Klimuk SK; Harasym TO; Dos Santos N; Ansell SM; Wong KF; Maurer N; Stark H; Cullis PR; Hope MJ; Scherrer P Efficient encapsulation of antisense oligonucleotides in lipid vesicles using ionizable aminolipids: formation of novel small multilamellar vesicle structures. Biochim. Biophys. Acta, 2001, 1510(1–2), 152–166. 10.1016/S0005-2736(00)00343-6 [PubMed: 11342155]

[31]. Adams D; Gonzalez-Duarte A; O'Riordan WD; Yang C-C; Ueda M; Kristen AV; Tournev I; Schmidt HH; Coelho T; Berk JL; Lin K-P; Vita G; Attarian S; Planté-Bordeneuve V; Mezei MM; Campistol JM; Buades J; Brannagan TH III; Kim BJ; Oh J; Parman Y; Sekijima Y; Hawkins PN; Solomon SD; Polydefkis M; Dyck PJ; Gandhi PJ; Goyal S; Chen J; Strahs AL; Nochur SV; Sweetser MT; Garg PP; Vaishnaw AK; Gollob JA; Suhr OB Patisiran, an RNAi Therapeutic, for Hereditary Transthyretin Amyloidosis. N. Engl. J. Med, 2018, 379(1), 11–21. 10.1056/NEJMoa1716153 [PubMed: 29972753]

[32]. Ickenstein LM; Garidel P Lipid-based nanoparticle formulations for small molecules and RNA drugs. Expert Opin. Drug Deliv, 2019, 16(11), 1205–1226. 10.1080/17425247.2019.1669558 [PubMed: 31530041]

[33]. Anselmo AC; Mitragotri S Nanoparticles in the clinic: An update. Bioeng. Transl. Med, 2019, 4(3)e10143 10.1002/btm2.10143 [PubMed: 31572799]

[34]. Ahmed KS; Hussein SA; Ali AH; Korma SA; Lipeng Q; Jinghua C Liposome: composition, characterisation, preparation, and recent innovation in clinical applications. J. Drug Target, 2019, 27(7), 742–761. 10.1080/1061186X.2018.1527337 [PubMed: 30239255]

[35]. Fenske DB; Cullis PR Liposomal nanomedicines. Expert Opin. Drug Deliv, 2008, 5(1), 25–44. 10.1517/17425247.5.1.25 [PubMed: 18095927]

[36]. Fenske DB; Chonn A; Cullis PR Liposomal nanomedicines: an emerging field. Toxicol. Pathol, 2008, 36(1), 21–29. 10.1177/0192623307310960 [PubMed: 18337218]

[37]. Puri A; Loomis K; Smith B; Lee J-H; Yavlovich A; Heldman E; Blumenthal R Lipid-based nanoparticles as pharmaceutical drug carriers: from concepts to clinic. Crit. Rev. Ther. Drug Carrier Syst, 2009, 26(6), 523–580. 10.1615/CritRevTherDrugCarrierSyst.v26.i6.10 [PubMed: 20402623]

[38]. Hattori Y; Suzuki S; Kawakami S; Yamashita F; Hashida M The role of dioleoylphosphatidylethanolamine (DOPE) in targeted gene delivery with mannosylated cationic liposomes via intravenous route. J. Control. Release, 2005, 108(2–3), 484–495. 10.1016/j.jconrel.2005.08.012 [PubMed: 16181701]

[39]. Edidin M Lipids on the frontier: a century of cell-membrane bilayers. Nat. Rev. Mol. Cell Biol, 2003, 4(5), 414–418. 10.1038/nrm1102 [PubMed: 12728275]

[40]. Shim G; Kim M-G; Park JY; Oh Y-K Application of Cationic Liposomes for Delivery of Nucleic Acids. Asian Journal of Pharmaceutical Sciences, 2013, 8, 72–80. 10.1016/j.ajps.2013.07.009

[41]. Kohli AG; Walsh CL; Szoka FC Synthesis and characterization of betaine-like diacyl lipids: zwitterionic lipids with the cationic amine at the bilayer interface. Chem. Phys. Lipids, 2012, 165(2), 252–259. 10.1016/j.chemphyslip.2012.01.005 [PubMed: 22301334]

[42]. Perttu EK; Szoka FC Jr Zwitterionic sulfobetaine lipids that form vesicles with salt-dependent thermotropic properties. Chem. Commun. (Camb.), 2011, 47(47), 12613–12615. 10.1039/c1cc15804j [PubMed: 22045250]

[43]. Luo C; Miao L; Zhao Y; Musetti S; Wang Y; Shi K; Huang L A novel cationic lipid with intrinsic antitumor activity to facilitate gene therapy of TRAIL DNA. Biomaterials, 2016, 102, 239–248. 10.1016/j.biomaterials.2016.06.030 [PubMed: 27344367]

[44]. Miao L; Li L; Huang Y; Delcassian D; Chahal J; Han J; Shi Y; Sadtler K; Gao W; Lin J; Doloff JC; Langer R; Anderson DG Delivery of mRNA vaccines with heterocyclic lipids increases anti-tumor efficacy by STING-mediated immune cell activation. Nat. Biotechnol, 2019, 37(10), 1174–1185. 10.1038/s41587-019-0247-3 [PubMed: 31570898]

[45]. Walsh CL; Nguyen J; Tiffany MR; Szoka FC Synthesis, characterization, and evaluation of ionizable lysine-based lipids for siRNA delivery. Bioconjug. Chem, 2013, 24(1), 36–43. 10.1021/bc300346h [PubMed: 23176544]

[46]. Zuhorn IS; Hoekstra D On the mechanism of cationic amphiphile-mediated transfection. To fuse or not to fuse: is that the question? J. Membr. Biol, 2002, 189(3), 167–179. 10.1007/s00232-002-1015-7 [PubMed: 12395282]

[47]. Zhi D; Bai Y; Yang J; Cui S; Zhao Y; Chen H; Zhang S A review on cationic lipids with different linkers for gene delivery. Adv. Colloid Interface Sci, 2018, 253, 117–140. 10.1016/j.cis.2017.12.006 [PubMed: 29454463]

[48]. Ramishetti S; Hazan-Halevy I; Palakuri R; Chatterjee S; Naidu Gonna S; Dammes N; Freilich I; Kolik Shmuel L; Danino D; Peer D A Combinatorial Library of Lipid Nanoparticles for RNA Delivery to Leukocytes. Adv. Mater, 2020, 32(12)e1906128 10.1002/adma.201906128 [PubMed: 31999380]

[49]. Zhi D; Zhang S; Wang B; Zhao Y; Yang B; Yu S Transfection efficiency of cationic lipids with different hydrophobic domains in gene delivery. Bioconjug. Chem, 2010, 21(4), 563–577. 10.1021/bc900393r [PubMed: 20121120]

[50]. Zhi D; Zhang S; Cui S; Zhao Y; Wang Y; Zhao D The headgroup evolution of cationic lipids for gene delivery. Bioconjug. Chem, 2013, 24(4), 487–519. 10.1021/bc300381s [PubMed: 23461774]

[51]. Hattori Y; Kawakami S; Suzuki S; Yamashita F; Hashida M Enhancement of immune responses by DNA vaccination through targeted gene delivery using mannosylated cationic liposome formulations following intravenous administration in mice. Biochem. Biophys. Res. Commun, 2004, 317(4), 992–999. 10.1016/j.bbrc.2004.03.141 [PubMed: 15094367]

[52]. Dow SW; Fradkin LG; Liggitt DH; Willson AP; Heath TD; Potter TA Lipid-DNA complexes induce potent activation of innate immune responses and antitumor activity when administered intravenously. J. Immunol, 1999, 163(3), 1552–1561. [PubMed: 10415059]

[53]. Pippa N; Pispas S; Demetzos C The delineation of the morphology of charged liposomal vectors via a fractal analysis in aqueous and biological media: physicochemical and self-assembly studies. Int. J. Pharm, 2012, 437(1–2), 264–274. 10.1016/j.ijpharm.2012.08.017 [PubMed: 22939965]

[54]. Heyes J; Palmer L; Bremner K; MacLachlan I Cationic lipid saturation influences intracellular delivery of encapsulated nucleic acids. J. Control. Release, 2005, 107(2), 276–287. 10.1016/j.jconrel.2005.06.014 [PubMed: 16054724]

[55]. Jayaraman M; Ansell SM; Mui BL; Tam YK; Chen J; Du X; Butler D; Eltepu L; Matsuda S; Narayanannair JK; Rajeev KG; Hafez IM; Akinc A; Maier MA; Tracy MA; Cullis PR; Madden TD; Manoharan M; Hope MJ Maximizing the potency of siRNA lipid nanoparticles for hepatic gene silencing *in vivo*. Angew. Chem. Int. Ed. Engl, 2012, 51(34), 8529–8533. 10.1002/anie.201203263 [PubMed: 22782619]

[56]. Alabi CA; Love KT; Sahay G; Yin H; Luly KM; Langer R; Anderson DG Multiparametric approach for the evaluation of lipid nanoparticles for siRNA delivery. Proc. Natl. Acad. Sci. USA, 2013, 110(32), 12881–12886. 10.1073/pnas.1306529110 [PubMed: 23882076]

[57]. Wang M; Zuris JA; Meng F; Rees H; Sun S; Deng P; Han Y; Gao X; Pouli D; Wu Q; Georgakoudi I; Liu DR; Xu Q Efficient delivery of genome-editing proteins using bioreducible lipid nanoparticles. Proc. Natl. Acad. Sci. USA, 2016, 113(11), 2868–2873. 10.1073/pnas.1520244113 [PubMed: 26929348]

[58]. Wei T; Cheng Q; Min Y-L.; Olson, E.N.; Siegwart, D.J. Systemic nanoparticle delivery of CRISPR-Cas9 ribonucleoproteins for effective tissue specific genome editing. Nat. Commun, 2020, 11(1), 3232. 10.1038/s41467-020-17029-3 [PubMed: 32591530]

[59]. Cheng Q; Wei T; Farbiak L; Johnson LT; Dilliard SA; Siegwart DJ Selective organ targeting (SORT) nanoparticles for tissue-specific mRNA delivery and CRISPR-Cas gene editing. Nat. Nanotechnol, 2020, 15(4), 313–320. 10.1038/s41565-020-0669-6 [PubMed: 32251383]

[60]. Cheng X; Lee RJ The role of helper lipids in lipid nanoparticles (LNPs) designed for oligonucleotide delivery. Adv. Drug Deliv. Rev, 2016, 99(Pt A), 129–137. 10.1016/j.addr.2016.01.022 [PubMed: 26900977]

[61]. Sakurai F; Nishioka T; Yamashita F; Takakura Y; Hashida M Effects of erythrocytes and serum proteins on lung accumulation of lipoplexes containing cholesterol or DOPE as a helper lipid in the single-pass rat lung perfusion system. Eur. J. Pharm. Biopharm, 2001, 52(2), 165–172. 10.1016/S0939-6411(01)00165-5 [PubMed: 11522482]

[62]. Scherphof G; Roerdink F; Waite M; Parks J Disintegration of phosphatidylcholine liposomes in plasma as a result of interaction with high-density lipoproteins. Biochim. Biophys. Acta, 1978, 542(2), 296–307. 10.1016/0304-4165(78)90025-9 [PubMed: 210837]

[63]. Patel S; Ashwanikumar N; Robinson E; Xia Y; Mihai C; Griffith JP III; Hou S; Esposito AA; Ketova T; Welsher K; Joyal JL; Almarsson Ö; Sahay G Naturally-occurring cholesterol analogues in lipid nanoparticles induce polymorphic shape and enhance intracellular delivery of mRNA. Nat. Commun, 2020, 11(1), 983. 10.1038/s41467-020-14527-2 [PubMed: 32080183]

[64]. Allen TM; Hansen C Pharmacokinetics of stealth versus conventional liposomes: effect of dose. Biochim. Biophys. Acta, 1991, 1068(2), 133–141. 10.1016/0005-2736(91)90201-I [PubMed: 1911826]

[65]. Kao YJ; Juliano RL Interactions of liposomes with the reticuloendothelial system. Effects of reticuloendothelial blockade on the clearance of large unilamellar vesicles. Biochim. Biophys. Acta, 1981, 677(3–4), 453–461. 10.1016/0304-4165(81)90259-2 [PubMed: 6895332]

[66]. Allen TM; Chonn A Large unilamellar liposomes with low uptake into the reticuloendothelial system. FEBS Lett, 1987, 223(1), 42–46. 10.1016/0014-5793(87)80506-9 [PubMed: 3666140]

[67]. Klibanov AL; Maruyama K; Torchilin VP; Huang L Amphipathic polyethyleneglycols effectively prolong the circulation time of liposomes. FEBS Lett, 1990, 268(1), 235–237. 10.1016/0014-5793(90)81016-H [PubMed: 2384160]

[68]. Blume G; Cevc G Liposomes for the Sustained Drug Release *in Vivo*. Biochimica et Biophysica Acta (BBA) −. Biomembranes, 1990, 1029, 91–97. 10.1016/0005-2736(90)90440-Y [PubMed: 2223816]

[69]. Jokerst JV; Lobovkina T; Zare RN; Gambhir SS Nanoparticle PEGylation for imaging and therapy. Nanomedicine (Lond.), 2011, 6(4), 715–728. 10.2217/nnm.11.19 [PubMed: 21718180]

[70]. Suk JS; Xu Q; Kim N; Hanes J; Ensign LM PEGylation as a strategy for improving nanoparticle-based drug and gene delivery. Adv. Drug Deliv. Rev, 2016, 99(Pt A), 28–51. 10.1016/j.addr.2015.09.012 [PubMed: 26456916]

[71]. Ryals RC; Patel S; Acosta C; McKinney M; Pennesi ME; Sahay G The effects of PEGylation on LNP based mRNA delivery to the eye. PLoS One, 2020, 15(10)e0241006 10.1371/journal.pone.0241006 [PubMed: 33119640]

[72]. Kohli AG; Kierstead PH; Venditto VJ; Walsh CL; Szoka FC Designer lipids for drug delivery: from heads to tails. J. Control. Release, 2014, 190, 274–287. 10.1016/j.jconrel.2014.04.047 [PubMed: 24816069]

[73]. Mahon KP; Love KT; Whitehead KA; Qin J; Akinc A; Leshchiner E; Leshchiner I; Langer R; Anderson DG Combinatorial approach to determine functional group effects on lipidoid-mediated siRNA delivery. Bioconjug. Chem, 2010, 21(8), 1448–1454. 10.1021/bc100041r [PubMed: 20715849]

[74]. Love KT; Mahon KP; Levins CG; Whitehead KA; Querbes W; Dorkin JR; Qin J; Cantley W; Qin LL; Racie T; Frank-Kamenetsky M; Yip KN; Alvarez R; Sah DWY; de Fougerolles A; Fitzgerald K; Koteliansky V; Akinc A; Langer R; Anderson DG Lipid-like materials for low-dose, *in vivo* gene silencing. Proc. Natl. Acad. Sci. USA, 2010, 107(5), 1864–1869. 10.1073/pnas.0910603106 [PubMed: 20080679]

[75]. Dong Y; Love KT; Dorkin JR; Sirirungruang S; Zhang Y; Chen D; Bogorad RL; Yin H; Chen Y; Vegas AJ; Alabi CA; Sahay G; Olejnik KT; Wang W; Schroeder A; Lytton-Jean AKR; Siegwart DJ; Akinc A; Barnes C; Barros SA; Carioto M; Fitzgerald K; Hettinger J; Kumar V; Novobrantseva TI; Qin J; Querbes W; Koteliansky V; Langer R; Anderson DG Lipopeptide nanoparticles for potent and selective siRNA delivery in rodents and nonhuman primates. Proc. Natl. Acad. Sci. USA, 2014, 111(11), 3955–3960. 10.1073/pnas.1322937111 [PubMed: 24516150]

[76]. Dong Y; Siegwart DJ; Anderson DG Strategies, design, and chemistry in siRNA delivery systems. Adv. Drug Deliv. Rev, 2019, 144, 133–147. 10.1016/j.addr.2019.05.004 [PubMed: 31102606]

[77]. Sanna V; Caria G; Mariani A Effect of Lipid Nanoparticles Containing Fatty Alcohols Having Different Chain Length on the Ex Vivo Skin Permeability of Econazole Nitrate. Powder Technol, 2010, 201, 32–36. 10.1016/j.powtec.2010.02.035

[78]. Wang M; Sun S; Alberti KA; Xu Q A combinatorial library of unsaturated lipidoids for efficient intracellular gene delivery. ACS Synth. Biol, 2012, 1(9), 403–407. 10.1021/sb300023h [PubMed: 23651337]

[79]. Altınoglu S; Wang M; Xu Q Combinatorial library strategies for synthesis of cationic lipid-like nanoparticles and their potential medical applications. Nanomedicine (Lond.), 2015, 10(4), 643–657. 10.2217/nnm.14.192 [PubMed: 25723096]

[80]. Hao J; Kos P; Zhou K; Miller JB; Xue L; Yan Y; Xiong H; Elkassih S; Siegwart DJ Rapid Synthesis of a Lipocationic Polyester Library via Ring-Opening Polymerization of Functional Valerolactones for Efficacious siRNA Delivery. J. Am. Chem. Soc, 2015, 137(29), 9206–9209. 10.1021/jacs.5b03429 [PubMed: 26166403]

[81]. Zhang X; Li B; Luo X; Zhao W; Jiang J; Zhang C; Gao M; Chen X; Dong Y Biodegradable Amino-Ester Nanomaterials for Cas9 mRNA Delivery *in Vitro* and *in Vivo*. ACS Appl. Mater. Interfaces, 2017, 9(30), 25481–25487. 10.1021/acsami.7b08163 [PubMed: 28685575]

[82]. Ball RL; Hajj KA; Vizelman J; Bajaj P; Whitehead KA Lipid Nanoparticle Formulations for Enhanced Co-delivery of siRNA and mRNA. Nano Lett, 2018, 18(6), 3814–3822. 10.1021/acs.nanolett.8b01101 [PubMed: 29694050]

[83]. Hajj KA; Ball RL; Deluty SB; Singh SR; Strelkova D; Knapp CM; Whitehead KA Branched-Tail Lipid Nanoparticles Potently Deliver mRNA *In Vivo* due to Enhanced Ionization at Endosomal pH. Small, 2019, 15(6)e1805097 10.1002/smll.201805097 [PubMed: 30637934]

[84]. Zhang X; Zhao W; Nguyen GN; Zhang C; Zeng C; Yan J; Du S; Hou X; Li W; Jiang J; Deng B; McComb DW; Dorkin R; Shah A; Barrera L; Gregoire F; Singh M; Chen D; Sabatino DE; Dong Y Functionalized lipid-like nanoparticles for *in vivo* mRNA delivery and base editing. Sci. Adv, 2020, 6(34)eabc2315 10.1126/sciadv.abc2315 [PubMed: 32937374]

[85]. Li B; Luo X; Deng B; Wang J; McComb DW; Shi Y; Gaensler KML; Tan X; Dunn AL; Kerlin BA; Dong Y An Orthogonal Array Optimization of Lipid-like Nanoparticles for mRNA Delivery *in Vivo*. Nano Lett, 2015, 15(12), 8099–8107. 10.1021/acs.nanolett.5b03528 [PubMed: 26529392]

[86]. Hou X; Zhang X; Zhao W; Zeng C; Deng B; McComb DW; Du S; Zhang C; Li W; Dong Y Vitamin lipid nanoparticles enable adoptive macrophage transfer for the treatment of multidrug-

resistant bacterial sepsis. Nat. Nanotechnol, 2020, 15(1), 41–46. 10.1038/s41565-019-0600-1 [PubMed: 31907443]

[87]. Kauffman KJ; Dorkin JR; Yang JH; Heartlein MW; DeRosa F; Mir FF; Fenton OS; Anderson DG Optimization of Lipid Nanoparticle Formulations for mRNA Delivery *in Vivo* with Fractional Factorial and Definitive Screening Designs. Nano Lett, 2015, 15(11), 7300–7306. 10.1021/acs.nanolett.5b02497 [PubMed: 26469188]

[88]. Cheng Q; Wei T; Jia Y; Farbiak L; Zhou K; Zhang S; Wei Y; Zhu H; Siegwart DJ Dendrimer-Based Lipid Nanoparticles Deliver Therapeutic FAH mRNA to Normalize Liver Function and Extend Survival in a Mouse Model of Hepatorenal Tyrosinemia Type I. Adv. Mater, 2018, 30(52)e1805308 10.1002/adma.201805308 [PubMed: 30368954]

[89]. Whitehead KA; Dorkin JR; Vegas AJ; Chang PH; Veiseh O; Matthews J; Fenton OS; Zhang Y; Olejnik KT; Yesilyurt V; Chen D; Barros S; Klebanov B; Novobrantseva T; Langer R; Anderson DG Degradable lipid nanoparticles with predictable *in vivo* siRNA delivery activity. Nat. Commun, 2014, 5, 4277. 10.1038/ncomms5277 [PubMed: 24969323]

[90]. Kulkarni JA; Witzigmann D; Chen S; Cullis PR; van der Meel R Lipid Nanoparticle Technology for Clinical Translation of siRNA Therapeutics. Acc. Chem. Res, 2019, 52(9), 2435–2444. 10.1021/acs.accounts.9b00368 [PubMed: 31397996]

[91]. Szoka F Jr; Papahadjopoulos D Procedure for preparation of liposomes with large internal aqueous space and high capture by reverse-phase evaporation. Proc. Natl. Acad. Sci. USA, 1978, 75(9), 4194–4198. 10.1073/pnas.75.9.4194 [PubMed: 279908]

[92]. Brunner J; Skrabal P; Hauser H Single bilayer vesicles prepared without sonication. Physico-chemical properties. Biochim. Biophys. Acta, 1976, 455(2), 322–331. 10.1016/0005-2736(76)90308-4 [PubMed: 1033769]

[93]. Bangham A; De Gier J; Greville G Osmotic Properties and Water Permeability of Phospholipid Liquid Crystals. Chem. Phys. Lipids, 1967, 1, 225–246. 10.1016/0009-3084(67)90030-8

[94]. Barenholzt Y; Amselem S; Lichtenberg D A new method for preparation of phospholipid vesicles (liposomes) - French press. FEBS Lett, 1979, 99(1), 210–214. 10.1016/0014-5793(79)80281-1 [PubMed: 437128]

[95]. Pick U Liposomes with a large trapping capacity prepared by freezing and thawing of sonicated phospholipid mixtures. Arch. Biochem. Biophys, 1981, 212(1), 186–194. 10.1016/0003-9861(81)90358-1 [PubMed: 7197900]

[96]. Magnan C; Badens E; Commenges N; Charbit G Soy Lecithin Micronization by Precipitation with a Compressed Fluid Antisolvent — Influence of Process Parameters. J. Supercrit. Fluids, 2000, 19, 69–77. 10.1016/S0896-8446(00)00076-0

[97]. El-Ali J; Sorger PK; Jensen KF Cells on chips. Nature, 2006, 442(7101), 403–411. 10.1038/nature05063 [PubMed: 16871208]

[98]. Yager P; Edwards T; Fu E; Helton K; Nelson K; Tam MR; Weigl BH Microfluidic diagnostic technologies for global public health. Nature, 2006, 442(7101), 412–418. 10.1038/nature05064 [PubMed: 16871209]

[99]. Yu B; Lee RJ; Lee LJ Chapter 7 - Microfluidic Methods for Production of Liposomes. Methods in Enzymology; Methods in Enzymology; Academic Press, 2009, 465, pp. 129–141. [PubMed: 19913165]

[100]. Leung AKK; Tam YYC; Chen S; Hafez IM; Cullis PR Microfluidic Mixing: A General Method for Encapsulating Macromolecules in Lipid Nanoparticle Systems. J. Phys. Chem. B, 2015, 119(28), 8698–8706. 10.1021/acs.jpcb.5b02891 [PubMed: 26087393]

[101]. Kim MS; Kim JS; Park HJ; Cho WK; Cha K-H; Hwang S-J Enhanced bioavailability of sirolimus via preparation of solid dispersion nanoparticles using a supercritical antisolvent process. Int. J. Nanomedicine, 2011, 6, 2997–3009. [PubMed: 22162657]

[102]. Otake K; Imura T; Sakai H; Abe M Development of a New Preparation Method of Liposomes Using Supercritical Carbon Dioxide. langmuir, 2001, 17, 3898–3901.

[103]. Otake K; Shimomura T; Goto T; Imura T; Furuya T; Yoda S; Takebayashi Y; Sakai H; Abe M Preparation of liposomes using an improved supercritical reverse phase evaporation method. Langmuir, 2006, 22(6), 2543–2550. 10.1021/la051654u [PubMed: 16519453]

[104]. Otake K; Shimomura T; Goto T; Imura T; Furuya T; Yoda S; Takebayashi Y; Sakai H; Abe M One-step preparation of chitosan-coated cationic liposomes by an improved supercritical reverse-phase evaporation method. Langmuir, 2006, 22(9), 4054–4059. 10.1021/la051662a [PubMed: 16618144]

[105]. Batzri S; Korn ED Single Bilayer Liposomes Prepared without Sonication. Biochimica et Biophysica Acta (BBA)-. Biomembranes, 1973, 298, 1015–1019. 10.1016/0005-2736(73)90408-2 [PubMed: 4738145]

[106]. Deamer D; Bangham A Large Volume Liposomes by an Ether Vaporization Method. Biochimica et Biophysica Acta (BBA)-. Biomembranes, 1976, 443, 629–634. 10.1016/0005-2736(76)90483-1 [PubMed: 963074]

[107]. Kremer JM; Esker MW; Pathmamanoharan C; Wiersema PH Vesicles of variable diameter prepared by a modified injection method. Biochemistry, 1977, 16(17), 3932–3935. 10.1021/bi00636a033 [PubMed: 901761]

[108]. Jaafar-Maalej C; Charcosset C; Fessi H A new method for liposome preparation using a membrane contactor. J. Liposome Res, 2011, 21(3), 213–220. 10.3109/08982104.2010.517537 [PubMed: 20860451]

[109]. Laouini A; Jaafar-Maalej C; Sfar S; Charcosset C; Fessi H Liposome preparation using a hollow fiber membrane contactor--application to spironolactone encapsulation. Int. J. Pharm, 2011, 415(1–2), 53–61. 10.1016/j.ijpharm.2011.05.034 [PubMed: 21641982]

[110]. Pham TT; Jaafar-Maalej C; Charcosset C; Fessi H Liposome and niosome preparation using a membrane contactor for scale-up. Colloids Surf. B Biointerfaces, 2012, 94, 15–21. 10.1016/j.colsurfb.2011.12.036 [PubMed: 22326648]

[111]. Jeffs LB; Palmer LR; Ambegia EG; Giesbrecht C; Ewanick S; MacLachlan I A scalable, extrusion-free method for efficient liposomal encapsulation of plasmid DNA. Pharm. Res, 2005, 22(3), 362–372. 10.1007/s11095-004-1873-z [PubMed: 15835741]

[112]. Zhang Y-P; Reimer DL; Zhang G; Lee PH; Bally MB Self-assembling DNA-lipid particles for gene transfer. Pharm. Res, 1997, 14(2), 190–196. 10.1023/A:1012000711033 [PubMed: 9090708]

[113]. Wheeler JJ; Palmer L; Ossanlou M; MacLachlan I; Graham RW; Zhang YP; Hope MJ; Scherrer P; Cullis PR Stabilized plasmid-lipid particles: construction and characterization. Gene Ther, 1999, 6(2), 271–281. 10.1038/sj.gt.3300821 [PubMed: 10435112]

[114]. Tam P; Monck M; Lee D; Ludkovski O; Leng EC; Clow K; Stark H; Scherrer P; Graham RW; Cullis PR Stabilized plasmid-lipid particles for systemic gene therapy. Gene Ther, 2000, 7(21), 1867–1874. 10.1038/sj.gt.3301308 [PubMed: 11110420]

[115]. Fenske DB; MacLachlan I; Cullis PR Stabilized plasmid-lipid particles: a systemic gene therapy vector. Methods Enzymol, 2002, 346, 36–71. 10.1016/S0076-6879(02)46048-X [PubMed: 11883080]

[116]. Belliveau NM; Huft J; Lin PJ; Chen S; Leung AK; Leaver TJ; Wild AW; Lee JB; Taylor RJ; Tam YK; Hansen CL; Cullis PR Microfluidic Synthesis of Highly Potent Limit-size Lipid Nanoparticles for *In Vivo* Delivery of siRNA. Mol. Ther. Nucleic Acids, 2012, 1e37 10.1038/mtna.2012.28 [PubMed: 23344179]

[117]. Chen D; Love KT; Chen Y; Eltoukhy AA; Kastrup C; Sahay G; Jeon A; Dong Y; Whitehead KA; Anderson DG Rapid discovery of potent siRNA-containing lipid nanoparticles enabled by controlled microfluidic formulation. J. Am. Chem. Soc, 2012, 134(16), 6948–6951. 10.1021/ja301621z [PubMed: 22475086]

[118]. Li B; Dong Y Preparation and Optimization of Lipid-Like Nanoparticles for MRNA Delivery. RNA Nanostructures : Methods and Protocols; Bindewald E; Shapiro BA, Eds.; Methods in Molecular Biology; Springer: New York, NY, 2017, pp. 207–217. 10.1007/978-1-4939-7138-1_13

[119]. Li Y; Lee RJ; Huang X; Li Y; Lv B; Wang T; Qi Y; Hao F; Lu J; Meng Q; Teng L; Zhou Y; Xie J; Teng L Single-step microfluidic synthesis of transferrin-conjugated lipid nanoparticles for siRNA delivery. Nanomedicine (Lond.), 2017, 13(2), 371–381. 10.1016/j.nano.2016.09.014

[120]. Hood RR; DeVoe DL High-Throughput Continuous Flow Production of Nanoscale Liposomes by Microfluidic Vertical Flow Focusing. small, 2015, 11, 5790–5799. [PubMed: 26395346]

[121]. Akbarzadeh A; Rezaei-Sadabady R; Davaran S; Joo SW; Zarghami N; Hanifehpour Y; Samiei M; Kouhi M; Nejati-Koshki K Liposome: classification, preparation, and applications. Nanoscale Res. Lett, 2013, 8(1), 102. 10.1186/1556-276X-8-102 [PubMed: 23432972]

[122]. Hwang SH; Maitani Y; Qi X-R; Takayama K; Nagai T Remote loading of diclofenac, insulin and fluorescein isothiocyanate labeled insulin into liposomes by pH and acetate gradient methods. Int. J. Pharm, 1999, 179(1), 85–95. 10.1016/S0378-5173(98)00392-5 [PubMed: 10053205]

[123]. Gabizon A; Shiota R; Papahadjopoulos D Pharmacokinetics and tissue distribution of doxorubicin encapsulated in stable liposomes with long circulation times. J. Natl. Cancer Inst, 1989, 81(19), 1484–1488. 10.1093/jnci/81.19.1484 [PubMed: 2778836]

[124]. Fenske DB; Wong KF; Maurer E; Maurer N; Leenhouts JM; Boman N; Amankwa L; Cullis PR Ionophore-mediated uptake of ciprofloxacin and vincristine into large unilamellar vesicles exhibiting transmembrane ion gradients. Biochim. Biophys. Acta, 1998, 1414(1–2), 188–204. 10.1016/S0005-2736(98)00166-7 [PubMed: 9804953]

[125]. Lasic DD; Frederik PM; Stuart MCA; Barenholz Y; McIntosh TJ Gelation of liposome interior. A novel method for drug encapsulation. FEBS Lett, 1992, 312(2–3), 255–258. 10.1016/0014-5793(92)80947-F [PubMed: 1426260]

[126]. Yu J; Zhou S; Li J; Wang Y; Su Y; Chi D; Wang J; Wang X; He Z; Lin G; Liu D; Wang Y Simple Weak-Acid Derivatives of Paclitaxel for Remote Loading into Liposomes and Improved Therapeutic Effects. RSC Advances, 2020, 10, 27676–27687. 10.1039/D0RA03190A

[127]. Ulrich AS Biophysical aspects of using liposomes as delivery vehicles. Biosci. Rep, 2002, 22(2), 129–150. 10.1023/A:1020178304031 [PubMed: 12428898]

[128]. Chen S; Tam YYC; Lin PJC; Sung MMH; Tam YK; Cullis PR Influence of particle size on the *in vivo* potency of lipid nanoparticle formulations of siRNA. J. Control. Release, 2016, 235, 236–244. 10.1016/j.jconrel.2016.05.059 [PubMed: 27238441]

[129]. Carr B; Wright M Nanoparticle Tracking Analysis. Innovations in Pharmaceutical Technology, 2008, 26, 38–40.

[130]. Hoo CM; Starostin N; West P; Mecartney ML A Comparison of Atomic Force Microscopy (AFM) and Dynamic Light Scattering (DLS) Methods to Characterize Nanoparticle Size Distributions. J. Nanopart. Res, 2008, 10, 89–96. 10.1007/s11051-008-9435-7

[131]. Wang H-X; Zuo Z-Q; Du J-Z; Wang Y-C; Sun R; Cao Z-T; Ye X-D; Wang J-L; Leong KW; Wang J Surface Charge Critically Affects Tumor Penetration and Therapeutic Efficacy of Cancer Nanomedicines. Nano Today, 2016, 11, 133–144. 10.1016/j.nantod.2016.04.008

[132]. Sousa Â; Almeida AM; Faria R; Konate K; Boisguerin P; Queiroz JA; Costa D Optimization of peptide-plasmid DNA vectors formulation for gene delivery in cancer therapy exploring design of experiments. Colloids Surf. B Biointerfaces, 2019, 183110417 10.1016/j.colsurfb.2019.110417 [PubMed: 31408780]

[133]. Hunter RJ; Midmore BR; Zhang H Zeta Potential of Highly Charged Thin Double-Layer Systems. J. Colloid Interface Sci, 2001, 237(1), 147–149. 10.1006/jcis.2001.7423 [PubMed: 11334528]

[134]. Schlieper P; Medda PK; Kaufmann R Drug-induced zeta potential changes in liposomes studied by laser Doppler spectroscopy. Biochim. Biophys. Acta, 1981, 644(2), 273–283. 10.1016/0005-2736(81)90385-0 [PubMed: 6114748]

[135]. Lin P-C; Lin S; Wang PC; Sridhar R Techniques for physicochemical characterization of nanomaterials. Biotechnol. Adv, 2014, 32(4), 711–726. 10.1016/j.biotechadv.2013.11.006 [PubMed: 24252561]

[136]. Kulkarni JA; Darjuan MM; Mercer JE; Chen S; van der Meel R; Thewalt JL; Tam YYC; Cullis PR On the Formation and Morphology of Lipid Nanoparticles Containing Ionizable Cationic Lipids and siRNA. ACS Nano, 2018, 12(5), 4787–4795. 10.1021/acsnano.8b01516 [PubMed: 29614232]

[137]. Kuntsche J; Horst JC; Bunjes H Cryogenic transmission electron microscopy (cryo-TEM) for studying the morphology of colloidal drug delivery systems. Int. J. Pharm, 2011, 417(1–2), 120–137. 10.1016/j.ijpharm.2011.02.001 [PubMed: 21310225]

[138]. Lasic DD Doxorubicin in sterically stabilized liposomes. Nature, 1996, 380(6574), 561–562. 10.1038/380561a0 [PubMed: 8606781]

[139]. Li X; Hirsh DJ; Cabral-Lilly D; Zirkel A; Gruner SM; Janoff AS; Perkins WR Doxorubicin physical state in solution and inside liposomes loaded via a pH gradient. Biochim. Biophys. Acta, 1998, 1415(1), 23–40. 10.1016/S0005-2736(98)00175-8 [PubMed: 9858673]

[140]. Gilleron J; Querbes W; Zeigerer A; Borodovsky A; Marsico G; Schubert U; Manygoats K; Seifert S; Andree C; Stöter M; Epstein-Barash H; Zhang L; Koteliansky V; Fitzgerald K; Fava E; Bickle M; Kalaidzidis Y; Akinc A; Maier M; Zerial M Image-based analysis of lipid nanoparticle-mediated siRNA delivery, intracellular trafficking and endosomal escape. Nat. Biotechnol, 2013, 31(7), 638–646. 10.1038/nbt.2612 [PubMed: 23792630]

[141]. Liu C; Zhao G; Liu J; Ma N; Chivukula P; Perelman L; Okada K; Chen Z; Gough D; Yu L Novel biodegradable lipid nano complex for siRNA delivery significantly improving the chemosensitivity of human colon cancer stem cells to paclitaxel. J. Control. Release, 2009, 140(3), 277–283. 10.1016/j.jconrel.2009.08.013 [PubMed: 19699770]

[142]. Li J; Chen Y-C; Tseng Y-C; Mozumdar S; Huang L Biodegradable calcium phosphate nanoparticle with lipid coating for systemic siRNA delivery. J. Control. Release, 2010, 142(3), 416–421. 10.1016/j.jconrel.2009.11.008 [PubMed: 19919845]

[143]. Billingsley MM; Singh N; Ravikumar P; Zhang R; June CH; Mitchell MJ Ionizable Lipid Nanoparticle-Mediated mRNA Delivery for Human CAR T Cell Engineering. Nano Lett, 2020, 20(3), 1578–1589. 10.1021/acs.nanolett.9b04246 [PubMed: 31951421]

[144]. Patel S; Ashwanikumar N; Robinson E; DuRoss A; Sun C; Murphy-Benenato KE; Mihai C; Almarsson Ö; Sahay G Boosting Intracellular Delivery of Lipid Nanoparticle-Encapsulated mRNA. Nano Lett, 2017, 17(9), 5711–5718. 10.1021/acs.nanolett.7b02664 [PubMed: 28836442]

[145]. Kaczmarek JC; Kauffman KJ; Fenton OS; Sadtler K; Patel AK; Heartlein MW; DeRosa F; Anderson DG Optimization of a Degradable Polymer-Lipid Nanoparticle for Potent Systemic Delivery of mRNA to the Lung Endothelium and Immune Cells. Nano Lett, 2018, 18(10), 6449–6454. 10.1021/acs.nanolett.8b02917 [PubMed: 30211557]

[146]. Zhao W; Zhang C; Li B; Zhang X; Luo X; Zeng C; Li W; Gao M; Dong Y Lipid Polymer Hybrid Nanomaterials for mRNA Delivery. Cell. Mol. Bioeng, 2018, 11(5), 397–406. 10.1007/s12195-018-0536-9 [PubMed: 30555598]

[147]. Yu X; Liu S; Cheng Q; Wei T; Lee S; Zhang D; Siegwart DJ Lipid-Modified Aminoglycosides for mRNA Delivery to the Liver. Adv. Healthc. Mater, 2020, 9(7)e1901487 10.1002/adhm.201901487 [PubMed: 32108440]

[148]. Jiang T; Xing B; Rao J Recent developments of biological reporter technology for detecting gene expression. Biotechnol. Genet. Eng. Rev, 2008, 25, 41–75. 10.5661/bger-25-41 [PubMed: 21412349]

[149]. Whitehead KA; Matthews J; Chang PH; Niroui F; Dorkin JR; Severgnini M; Anderson DG *In vitro-in vivo* translation of lipid nanoparticles for hepatocellular siRNA delivery. ACS Nano, 2012, 6(8), 6922–6929. 10.1021/nn301922x [PubMed: 22770391]

[150]. Lokugamage MP; Sago CD; Dahlman JE Testing thousands of nanoparticles *in vivo* using DNA barcodes. Curr Opin Biomed Eng, 2018, 7, 1–8. 10.1016/j.cobme.2018.08.001 [PubMed: 30931416]

[151]. Paunovska K; Da Silva Sanchez AJ; Sago CD; Gan Z; Lokugamage MP; Islam FZ; Kalathoor S; Krupczak BR; Dahlman JE Nanoparticles Containing Oxidized Cholesterol Deliver mRNA to the Liver Microenvironment at Clinically Relevant Doses. Adv. Mater, 2019, 31(14)e1807748 10.1002/adma.201807748 [PubMed: 30748040]

[152]. Sago CD; Lokugamage MP; Paunovska K; Vanover DA; Monaco CM; Shah NN; Gamboa Castro M; Anderson SE; Rudoltz TG; Lando GN; Munnilal Tiwari P; Kirschman JL; Willett N; Jang YC; Santangelo PJ; Bryksin AV; Dahlman JE High-throughput *in vivo* screen of functional mRNA delivery identifies nanoparticles for endothelial cell gene editing. Proc. Natl. Acad. Sci. USA, 2018, 115(42), E9944–E9952. 10.1073/pnas.1811276115 [PubMed: 30275336]

[153]. Dahlman JE; Kauffman KJ; Xing Y; Shaw TE; Mir FF; Dlott CC; Langer R; Anderson DG; Wang ET Barcoded nanoparticles for high throughput *in vivo* discovery of targeted therapeutics. Proc. Natl. Acad. Sci. USA, 2017, 114(8), 2060–2065. 10.1073/pnas.1620874114 [PubMed: 28167778]

[154]. Guimaraes PPG; Zhang R; Spektor R; Tan M; Chung A; Billingsley MM; El-Mayta R; Riley RS; Wang L; Wilson JM; Mitchell MJ Ionizable lipid nanoparticles encapsulating barcoded mRNA for accelerated *in vivo* delivery screening. J. Control. Release, 2019, 316, 404–417. 10.1016/j.jconrel.2019.10.028 [PubMed: 31678653]

[155]. Frenkel D; Smit B Understanding Molecular Simulation; From Algorithms to Applications; Academic Press, 2001.

[156]. Gooneie A; Schuschnigg S; Holzer C A Review of Multiscale Computational Methods in Polymeric Materials. Polymers (Basel), 2017, 9(1), 16. 10.3390/polym9010016

[157]. Sherwood P; Brooks BR; Sansom MS Multiscale methods for macromolecular simulations. Curr. Opin. Struct. Biol, 2008, 18(5), 630–640. 10.1016/j.sbi.2008.07.003 [PubMed: 18721882]

[158]. Meier K; Choutko A; Dolenc J; Eichenberger AP; Riniker S; van Gunsteren WF Multi-resolution simulation of biomolecular systems: a review of methodological issues. Angew. Chem. Int. Ed. Engl, 2013, 52(10), 2820–2834. 10.1002/anie.201205408 [PubMed: 23417997]

[159]. Dickson CJ; Madej BD; Skjevik ÅA; Betz RM; Teigen K; Gould IR; Walker RC Lipid14: The Amber Lipid Force Field. J. Chem. Theory Comput, 2014, 10(2), 865–879. 10.1021/ct4010307 [PubMed: 24803855]

[160]. Huang J; Rauscher S; Nawrocki G; Ran T; Feig M; de Groot BL; Grubmüller H; MacKerell AD Jr CHARMM36m: an improved force field for folded and intrinsically disordered proteins. Nat. Methods, 2017, 14(1), 71–73. 10.1038/nmeth.4067 [PubMed: 27819658]

[161]. Klauda JB; Venable RM; Freites JA; O'Connor JW; Tobias DJ; Mondragon-Ramirez C; Vorobyov I; MacKerell AD Jr; Pastor RW Update of the CHARMM all-atom additive force field for lipids: validation on six lipid types. J. Phys. Chem. B, 2010, 114(23), 7830–7843. 10.1021/jp101759q [PubMed: 20496934]

[162]. Hart K; Foloppe N; Baker CM; Denning EJ; Nilsson L; Mackerell AD Jr Optimization of the CHARMM additive force field for DNA: Improved treatment of the BI/BII conformational equilibrium. J. Chem. Theory Comput, 2012, 8(1), 348–362. 10.1021/ct200723y [PubMed: 22368531]

[163]. Denning EJ; Priyakumar UD; Nilsson L; Mackerell AD Jr Impact of 2′-hydroxyl sampling on the conformational properties of RNA: update of the CHARMM all-atom additive force field for RNA. J. Comput. Chem, 2011, 32(9), 1929–1943. 10.1002/jcc.21777 [PubMed: 21469161]

[164]. Siu SWI; Pluhackova K; Böckmann RA Optimization of the OPLS-AA Force Field for Long Hydrocarbons. J. Chem. Theory Comput, 2012, 8(4), 1459–1470. 10.1021/ct200908r [PubMed: 26596756]

[165]. Sun D; Forsman J; Woodward CE Evaluating Force Fields for the Computational Prediction of Ionized Arginine and Lysine Side-Chains Partitioning into Lipid Bilayers and Octanol. J. Chem. Theory Comput, 2015, 11(4), 1775–1791. 10.1021/ct501063a [PubMed: 26574387]

[166]. Best RB; Hofmann H; Nettels D; Schuler B Quantitative interpretation of FRET experiments via molecular simulation: force field and validation. Biophys. J, 2015, 108(11), 2721–2731. 10.1016/j.bpj.2015.04.038 [PubMed: 26039173]

[167]. Brooks BR; Brooks CL III; Mackerell AD Jr; Nilsson L; Petrella RJ; Roux B; Won Y; Archontis G; Bartels C; Boresch S; Caflisch A; Caves L; Cui Q; Dinner AR; Feig M; Fischer S; Gao J; Hodoscek M; Im W; Kuczera K; Lazaridis T; Ma J; Ovchinnikov V; Paci E; Pastor RW; Post CB; Pu JZ; Schaefer M; Tidor B; Venable RM; Woodcock HL; Wu X; Yang W; York DM; Karplus M CHARMM: the biomolecular simulation program. J. Comput. Chem, 2009, 30(10), 1545–1614. 10.1002/jcc.21287 [PubMed: 19444816]

[168]. Case DA; Cheatham TE III; Darden T; Gohlke H; Luo R; Merz KM Jr; Onufriev A; Simmerling C; Wang B; Woods RJ The Amber biomolecular simulation programs. J. Comput. Chem, 2005, 26(16), 1668–1688. 10.1002/jcc.20290 [PubMed: 16200636]

[169]. Phillips JC; Braun R; Wang W; Gumbart J; Tajkhorshid E; Villa E; Chipot C; Skeel RD; Kalé L; Schulten K Scalable molecular dynamics with NAMD. J. Comput. Chem, 2005, 26(16), 1781–1802. 10.1002/jcc.20289 [PubMed: 16222654]

[170]. Abraham MJ; Murtola T; Schulz R; Páll S; Smith JC; Hess B; Lindahl E GROMACS: High Performance Molecular Simulations through Multi-Level Parallelism from Laptops to Supercomputers. SoftwareX, 2015, 1–2, 19–25. 10.1016/j.softx.2015.06.001

[171]. Eastman P; Swails J; Chodera JD; McGibbon RT; Zhao Y; Beauchamp KA; Wang L-P; Simmonett AC; Harrigan MP; Stern CD; Wiewiora RP; Brooks BR; Pande VS OpenMM 7: Rapid development of high performance algorithms for molecular dynamics. PLOS Comput. Biol, 2017, 13(7)e1005659 10.1371/journal.pcbi.1005659 [PubMed: 28746339]

[172]. Plimpton S Fast Parallel Algorithms for Short-Range Molecular Dynamics. J. Comput. Phys, 1995, 117, 1–19. 10.1006/jcph.1995.1039

[173]. Marrink SJ; Tieleman DP Perspective on the Martini model. Chem. Soc. Rev, 2013, 42(16), 6801–6822. 10.1039/c3cs60093a [PubMed: 23708257]

[174]. Pak AJ; Voth GA Advances in coarse-grained modeling of macromolecular complexes. Curr. Opin. Struct. Biol, 2018, 52, 119–126. 10.1016/j.sbi.2018.11.005 [PubMed: 30508766]

[175]. Lu L; Dama JF; Voth GA Fitting coarse-grained distribution functions through an iterative force-matching method. J. Chem. Phys, 2013, 139(12)121906 10.1063/1.4811667 [PubMed: 24089718]

[176]. Izvekov S; Voth GA Effective force field for liquid hydrogen fluoride from ab initio molecular dynamics simulation using the force-matching method. J. Phys. Chem. B, 2005, 109(14), 6573–6586. 10.1021/jp0456685 [PubMed: 16851738]

[177]. Lyman E; Pfaendtner J; Voth GA Systematic multiscale parameterization of heterogeneous elastic network models of proteins. Biophys. J, 2008, 95(9), 4183–4192. 10.1529/biophysj.108.139733 [PubMed: 18658214]

[178]. Lu L; Voth GA Systematic coarse-graining of a multicomponent lipid bilayer. J. Phys. Chem. B, 2009, 113(5), 1501–1510. 10.1021/jp809604k [PubMed: 19138138]

[179]. Izvekov S; Voth GA Solvent-free lipid bilayer model using multiscale coarse-graining. J. Phys. Chem. B, 2009, 113(13), 4443–4455. 10.1021/jp810440c [PubMed: 19267467]

[180]. Chu J-W; Izveko S; Voth GA The Multiscale Challenge for Biomolecular Systems: Coarse-Grained Modeling. Mol. Simul, 2006, 32, 211–218. 10.1080/08927020600612221

[181]. Grime JMA; Dama JF; Ganser-Pornillos BK; Woodward CL; Jensen GJ; Yeager M; Voth GA Coarse-grained simulation reveals key features of HIV-1 capsid self-assembly. Nat. Commun, 2016, 7, 11568. 10.1038/ncomms11568 [PubMed: 27174390]

[182]. Noguchi H; Takasu M Adhesion of nanoparticles to vesicles: a Brownian dynamics simulation. Biophys. J, 2002, 83(1), 299–308. 10.1016/S0006-3495(02)75170-9 [PubMed: 12080121]

[183]. Noguchi H; Takasu M Structural changes of pulled vesicles: a Brownian dynamics simulation. Phys. Rev. E Stat. Nonlin. Soft Matter Phys, 2002, 65(5 Pt 1)051907 10.1103/PhysRevE.65.051907 [PubMed: 12059593]

[184]. Goga N; Rzepiela AJ; de Vries AH; Marrink SJ; Berendsen HJC Efficient Algorithms for Langevin and DPD Dynamics. J. Chem. Theory Comput, 2012, 8(10), 3637–3649. 10.1021/ct3000876 [PubMed: 26593009]

[185]. Moeendarbary E; Ng TY; Zangeneh M DISSIPATIVE PARTICLE DYNAMICS: INTRODUCTION, METHODOLOGY AND COMPLEX FLUID APPLICATIONS — A REVIEW. Int. J. Appl. Mech, 2009, 01, 737–763. 10.1142/S1758825109000381

[186]. Sadeghi M; Noé F Large-scale simulation of biomembranes incorporating realistic kinetics into coarse-grained models. Nat. Commun, 2020, 11(1), 2951. 10.1038/s41467-020-16424-0 [PubMed: 32528158]

[187]. Pezeshkian W; König M; Wassenaar TA; Marrink SJ Backmapping triangulated surfaces to coarse-grained membrane models. Nat. Commun, 2020, 11(1), 2296. 10.1038/s41467-020-16094-y [PubMed: 32385270]

[188]. Simunovic M; Evergren E; Golushko I; Prévost C; Renard H-F; Johannes L; McMahon HT; Lorman V; Voth GA; Bassereau P How curvature-generating proteins build scaffolds on membrane nanotubes. Proc. Natl. Acad. Sci. USA, 2016, 113(40), 11226–11231. 10.1073/pnas.1606943113 [PubMed: 27655892]

[189]. Davtyan A; Simunovic M; Voth GA The mesoscopic membrane with proteins (MesM-P) model. J. Chem. Phys, 2017, 147(4)044101 10.1063/1.4993514 [PubMed: 28764362]

[190]. Bahrami AH; Lipowsky R; Weikl TR Tubulation and aggregation of spherical nanoparticles adsorbed on vesicles. Phys. Rev. Lett, 2012, 109(18)188102 10.1103/PhysRevLett.109.188102 [PubMed: 23215335]

[191]. Hoore M; Yaya F; Podgorski T; Wagner C; Gompper G; Fedosov DA Effect of spectrin network elasticity on the shapes of erythrocyte doublets. Soft Matter, 2018, 14(30), 6278–6289. 10.1039/C8SM00634B [PubMed: 30014074]

[192]. Cournia Z; Ullmann GM; Smith JC Differential effects of cholesterol, ergosterol and lanosterol on a dipalmitoyl phosphatidylcholine membrane: a molecular dynamics simulation study. J. Phys. Chem. B, 2007, 111(7), 1786–1801. 10.1021/jp065172i [PubMed: 17261058]

[193]. Pan J; Cheng X; Heberle FA; Mostofian B; Kučerka N; Drazba P; Katsaras J Interactions between ether phospholipids and cholesterol as determined by scattering and molecular dynamics simulations. J. Phys. Chem. B, 2012, 116(51), 14829–14838. 10.1021/jp310345j [PubMed: 23199292]

[194]. Sodt AJ; Sandar ML; Gawrisch K; Pastor RW; Lyman E The molecular structure of the liquid-ordered phase of lipid bilayers. J. Am. Chem. Soc, 2014, 136(2), 725–732. 10.1021/ja4105667 [PubMed: 24345334]

[195]. Johnson QR; Mostofian B; Fuente Gomez G; Smith JC; Cheng X Effects of carotenoids on lipid bilayers. Phys. Chem. Chem. Phys, 2018, 20(5), 3795–3804. 10.1039/C7CP07126D [PubMed: 29349456]

[196]. Mostofian B; Johnson QR; Smith JC; Cheng X Carotenoids promote lateral packing and condensation of lipid membranes. Phys. Chem. Chem. Phys, 2020, 22(21), 12281–12293. 10.1039/D0CP01031F [PubMed: 32432296]

[197]. McClements DJ Enhanced delivery of lipophilic bioactives using emulsions: a review of major factors affecting vitamin, nutraceutical, and lipid bioaccessibility. Food Funct, 2018, 9(1), 22–41. 10.1039/C7FO01515A [PubMed: 29119979]

[198]. Atkinson J; Harroun T; Wassall SR; Stillwell W; Katsaras J The location and behavior of α-tocopherol in membranes. Mol. Nutr. Food Res, 2010, 54(5), 641–651. 10.1002/mnfr.200900439 [PubMed: 20166146]

[199]. Cheng X; Smith JC Biological Membrane Organization and Cellular Signaling. Chem. Rev, 2019, 119(9), 5849–5880. 10.1021/acs.chemrev.8b00439 [PubMed: 30747526]

[200]. Merz KM, Jr Molecular dynamics simulations of lipid bilayers. Curr. Opin. Struct. Biol, 1997, 7(4), 511–517. 10.1016/S0959-440X(97)80115-7 [PubMed: 9266172]

[201]. Merz KM; Roux B Biological Membranes: A Molecular Perspective from Computation and Experiment; Springer Science & Business Media, 2012.

[202]. Marrink S-J; Berendsen HJC Simulation of Water Transport through a Lipid Membrane. J. Phys. Chem, 1994, 98, 4155–4168. 10.1021/j100066a040

[203]. Marrink SJ; Berendsen HJC Permeation Process of Small Molecules across Lipid Membranes Studied by Molecular Dynamics Simulations. J. Phys. Chem, 1996, 100, 16729–16738. 10.1021/jp952956f

[204]. Bemporad D; Luttmann C; Essex JW Computer simulation of small molecule permeation across a lipid bilayer: dependence on bilayer properties and solute volume, size, and cross-sectional area. Biophys. J, 2004, 87(1), 1–13. 10.1529/biophysj.103.030601 [PubMed: 15240439]

[205]. Bemporad D; Essex JW; Luttmann C Permeation of Small Molecules through a Lipid Bilayer: A Computer Simulation Study. J. Phys. Chem. B, 2004, 108, 4875–4884. 10.1021/jp035260s

[206]. Zhang H; Shao X; Dehez F; Cai W; Chipot C Modulation of membrane permeability by carbon dioxide. J. Comput. Chem, 2020, 41(5), 421–426. 10.1002/jcc.26063 [PubMed: 31479166]

[207]. Comer J; Schulten K; Chipot C Permeability of a Fluid Lipid Bilayer to Short-Chain Alcohols from First Principles. Journal of Chemical Theory and Computation, 2017. 10.1021/acs.jctc.7b00264

[208]. Chipot C; Comer J Subdiffusion in Membrane Permeation of Small Molecules. Sci. Rep, 2016, 6, 35913. 10.1038/srep35913 [PubMed: 27805049]

[209]. Tse CH; Comer J; Sang Chu SK; Wang Y; Chipot C Affordable Membrane Permeability Calculations: Permeation of Short-Chain Alcohols through Pure-Lipid Bilayers and a Mammalian Cell Membrane. J. Chem. Theory Comput, 2019, 15(5), 2913–2924. 10.1021/acs.jctc.9b00022 [PubMed: 30998342]

[210]. Comer J; Chipot C; González-Nilo FD Calculating Position-Dependent Diffusivity in Biased Molecular Dynamics Simulations. J. Chem. Theory Comput, 2013, 9(2), 876–882. 10.1021/ct300867e [PubMed: 26588731]

[211]. Comer J; Gumbart JC; Hénin J; Lelièvre T; Pohorille A; Chipot C The Adaptive Biasing Force Method: Everything You Always Wanted To Know but Were Afraid To Ask. The Journal of Physical Chemistry B, 2014.

[212]. Martinotti C; Ruiz-Perez L; Deplazes E; Mancera RL Molecular Dynamics Simulation of the Interaction of Small Molecules with Biological Membranes. ChemPhysChem, 2020.

[213]. Venable RM; Krämer A; Pastor RW Molecular Dynamics Simulations of Membrane Permeability. Chem. Rev, 2019, 119(9), 5954–5997. 10.1021/acs.chemrev.8b00486 [PubMed: 30747524]

[214]. Dzieciuch M; Rissanen S; Szydłowska N; Bunker A; Kumorek M; Jamróz D; Vattulainen I; Nowakowska M; Róg T; Kepczynski M PEGylated Liposomes as Carriers of Hydrophobic Porphyrins. J. Phys. Chem. B, 2015, 119(22), 6646–6657. 10.1021/acs.jpcb.5b01351 [PubMed: 25965670]

[215]. Lehtinen J; Magarkar A; Stepniewski M; Hakola S; Bergman M; Róg T; Yliperttula M; Urtti A; Bunker A Analysis of cause of failure of new targeting peptide in PEGylated liposome: molecular modeling as rational design tool for nanomedicine. Eur. J. Pharm. Sci, 2012, 46(3), 121–130. 10.1016/j.ejps.2012.02.009 [PubMed: 22381076]

[216]. Li Y-C; Rissanen S; Stepniewski M; Cramariuc O; Róg T; Mirza S; Xhaard H; Wytrwal M; Kepczynski M; Bunker A Study of interaction between PEG carrier and three relevant drug molecules: piroxicam, paclitaxel, and hematoporphyrin. J. Phys. Chem. B, 2012, 116(24), 7334–7341. 10.1021/jp300301z [PubMed: 22587534]

[217]. Vuković L; Khatib FA; Drake SP; Madriaga A; Brandenburg KS; Král P; Onyuksel H Structure and dynamics of highly PEGylated sterically stabilized micelles in aqueous media. J. Am. Chem. Soc, 2011, 133(34), 13481–13488. 10.1021/ja204043b [PubMed: 21780810]

[218]. Vuković L; Madriaga A; Kuzmis A; Banerjee A; Tang A; Tao K; Shah N; Král P; Onyuksel H Solubilization of therapeutic agents in micellar nanomedicines. Langmuir, 2013, 29(51), 15747–15754. 10.1021/la403264w [PubMed: 24283508]

[219]. Magarkar A; Róg T; Bunker A Molecular Dynamics Simulation of PEGylated Membranes with Cholesterol: Building Toward the DOXIL Formulation. J. Phys. Chem. C, 2014, 118, 15541–15549. 10.1021/jp504962m

[220]. Eriksson ESE; Eriksson LA The Influence of Cholesterol on the Properties and Permeability of Hypericin Derivatives in Lipid Membranes. J. Chem. Theory Comput, 2011, 7(3), 560–574. 10.1021/ct100528u [PubMed: 26596290]

[221]. Khelashvili G; Harries D How cholesterol tilt modulates the mechanical properties of saturated and unsaturated lipid membranes. J. Phys. Chem. B, 2013, 117(8), 2411–2421. 10.1021/jp3122006 [PubMed: 23323733]

[222]. Magarkar A; Karakas E; Stepniewski M; Róg T; Bunker A Molecular dynamics simulation of PEGylated bilayer interacting with salt ions: a model of the liposome surface in the bloodstream. J. Phys. Chem. B, 2012, 116(14), 4212–4219. 10.1021/jp300184z [PubMed: 22420691]

[223]. Stepniewski M; Pasenkiewicz-Gierula M; Róg T; Danne R; Orlowski A; Karttunen M; Urtti A; Yliperttula M; Vuorimaa E; Bunker A Study of PEGylated lipid layers as a model for PEGylated liposome surfaces: molecular dynamics simulation and Langmuir monolayer studies. Langmuir, 2011, 27(12), 7788–7798. 10.1021/la200003n [PubMed: 21604684]

[224]. Bunker A; Magarkar A; Viitala T Rational design of liposomal drug delivery systems, a review: Combined experimental and computational studies of lipid membranes, liposomes and their PEGylation. Biochim. Biophys. Acta, 2016, 1858(10), 2334–2352. 10.1016/j.bbamem.2016.02.025 [PubMed: 26915693]

[225]. Nosova AS; Koloskova OO; Nikonova AA; Simonova VA; Smirnov VV; Kudlay D; Khaitov MR Diversity of PEGylation methods of liposomes and their influence on RNA delivery. MedChemComm, 2019, 10(3), 369–377. 10.1039/C8MD00515J [PubMed: 31015904]

[226]. Sousa SF; Peres J; Coelho M; Vieira TF Analyzing PEGylation through Molecular Dynamics Simulations. ChemistrySelect, 2018, 3, 8415–8427. 10.1002/slct.201800855

[227]. Irby D; Du C; Li F Lipid-Drug Conjugate for Enhancing Drug Delivery. Mol. Pharm, 2017, 14(5), 1325–1338. 10.1021/acs.molpharmaceut.6b01027 [PubMed: 28080053]

[228]. Ramezanpour M; Leung SSW; Delgado-Magnero KH; Bashe BYM; Thewalt J; Tieleman DP Computational and experimental approaches for investigating nanoparticle-based drug delivery systems. Biochim. Biophys. Acta, 2016, 1858(7 Pt B), 1688–1709. 10.1016/j.bbamem.2016.02.028 [PubMed: 26930298]

[229]. Wang P; Ma Y; Liu Z; Yan Y; Sun X; Zhang J Vesicle Formation of Catanionic Mixtures of CTAC/SDS Induced by Ratio: A Coarse-Grained Molecular Dynamic Simulation Study. RSC Advances, 2016, 6, 13442–13449. 10.1039/C5RA26051E

[230]. Marrink SJ; Mark AE Molecular dynamics simulation of the formation, structure, and dynamics of small phospholipid vesicles. J. Am. Chem. Soc, 2003, 125(49), 15233–15242. 10.1021/ja0352092 [PubMed: 14653758]

[231]. Chng C-P Effect of Simulation Temperature on Phospholipid Bilayer-Vesicle Transition Studied by Coarse-Grained Molecular Dynamics Simulations. Soft Matter, 2013, 9, 7294–7301. 10.1039/c3sm51038g

[232]. Sun X-L; Pei S; Wang J-F; Wang P; Liu Z-B; Zhang J Coarse-Grained Molecular Dynamics Simulation Study on Spherical and Tube-like Vesicles Formed by Amphiphilic Copolymers. J. Polym. Sci., B, Polym. Phys, 2017, 55, 1220–1226. 10.1002/polb.24376

[233]. de Vries AH; Mark AE; Marrink SJ Molecular dynamics simulation of the spontaneous formation of a small DPPC vesicle in water in atomistic detail. J. Am. Chem. Soc, 2004, 126(14), 4488–4489. 10.1021/ja0398417 [PubMed: 15070345]

[234]. Parchekani Choozaki J; Taghdir M Investigation the Effect of Cholesterol on the Formation and Stability of the Liposomes Using Coarse-Grained Molecular Dynamics Simulations. Modares Journal of Biotechnology, 2019, 10, 241–246.

[235]. Koshiyama K; Wada S Collapse of a lipid-coated nanobubble and subsequent liposome formation. Sci. Rep, 2016, 6, 28164. 10.1038/srep28164 [PubMed: 27306704]

[236]. Knecht V; Marrink S-J Molecular dynamics simulations of lipid vesicle fusion in atomic detail. Biophys. J, 2007, 92(12), 4254–4261. 10.1529/biophysj.106.103572 [PubMed: 17384060]

[237]. Marrink SJ; Mark AE The mechanism of vesicle fusion as revealed by molecular dynamics simulations. J. Am. Chem. Soc, 2003, 125(37), 11144–11145. 10.1021/ja036138+ [PubMed: 16220905]

[238]. Pannuzzo M; De Jong DH; Raudino A; Marrink SJ Simulation of polyethylene glycol and calcium-mediated membrane fusion. J. Chem. Phys, 2014, 140(12)124905 10.1063/1.4869176 [PubMed: 24697479]

[239]. Venable RM; Ingólfsson HI; Lerner MG; Perrin BS Jr; Camley BA; Marrink SJ; Brown FLH; Pastor RW Lipid and Peptide Diffusion in Bilayers: The Saffman-Delbrück Model and Periodic Boundary Conditions. J. Phys. Chem. B, 2017, 121(15), 3443–3457. 10.1021/acs.jpcb.6b09111 [PubMed: 27966982]

[240]. Baoukina S; Tieleman DP Direct simulation of protein-mediated vesicle fusion: lung surfactant protein B. Biophys. J, 2010, 99(7), 2134–2142. 10.1016/j.bpj.2010.07.049 [PubMed: 20923647]

[241]. Li Y; Li X; Li Z; Gao H Surface-structure-regulated penetration of nanoparticles across a cell membrane. Nanoscale, 2012, 4(12), 3768–3775. 10.1039/c2nr30379e [PubMed: 22609866]

[242]. Chen L; Wu Z; Wu X; Liao Y; Dai X; Shi X The Application of Coarse-Grained Molecular Dynamics to the Evaluation of Liposome Physical Stability. AAPS PharmSciTech, 2020, 21(5), 138. 10.1208/s12249-020-01680-6 [PubMed: 32419093]

[243]. Tamai H; Okutsu N; Tokuyama Y; Shimizu E; Miyagi S; Shulga S; Danilov VI; Kurita N A Coarse Grained Molecular Dynamics Study on the Structure and Stability of Small-Sized Liposomes. Mol. Simul, 2016, 42, 122–130. 10.1080/08927022.2015.1020487

[244]. Risselada HJ; Marrink SJ; Müller M Curvature-dependent elastic properties of liquid-ordered domains result in inverted domain sorting on uniaxially compressed vesicles. Phys. Rev. Lett, 2011, 106(14)148102 10.1103/PhysRevLett.106.148102 [PubMed: 21561224]

[245]. Risselada HJ; Marrink SJ Curvature effects on lipid packing and dynamics in liposomes revealed by coarse grained molecular dynamics simulations. Phys. Chem. Chem. Phys, 2009, 11(12), 2056–2067. 10.1039/b818782g [PubMed: 19280016]

[246]. Semple SC; Akinc A; Chen J; Sandhu AP; Mui BL; Cho CK; Sah DWY; Stebbing D; Crosley EJ; Yaworski E; Hafez IM; Dorkin JR; Qin J; Lam K; Rajeev KG; Wong KF; Jeffs LB; Nechev L; Eisenhardt ML; Jayaraman M; Kazem M; Maier MA; Srinivasulu M; Weinstein MJ; Chen Q; Alvarez R; Barros SA; De S; Klimuk SK; Borland T; Kosovrasti V; Cantley WL; Tam YK; Manoharan M; Ciufolini MA; Tracy MA; de Fougerolles A; MacLachlan I; Cullis PR; Madden TD; Hope MJ Rational design of cationic lipids for siRNA delivery. Nat. Biotechnol, 2010, 28(2), 172–176. 10.1038/nbt.1602 [PubMed: 20081866]

[247]. Jämbeck JPM; Eriksson ESE; Laaksonen A; Lyubartsev AP; Eriksson LA Molecular Dynamics Studies of Liposomes as Carriers for Photosensitizing Drugs: Development, Validation, and Simulations with a Coarse-Grained Model. J. Chem. Theory Comput, 2014, 10(1), 5–13. 10.1021/ct400466m [PubMed: 26579887]

[248]. Genheden S; Eriksson LA Estimation of Liposome Penetration Barriers of Drug Molecules with All-Atom and Coarse-Grained Models. J. Chem. Theory Comput, 2016, 12(9), 4651–4661. 10.1021/acs.jctc.6b00557 [PubMed: 27541708]

[249]. Pickholz M; Giupponi G Coarse grained simulations of local anesthetics encapsulated into a liposome. J. Phys. Chem. B, 2010, 114(20), 7009–7015. 10.1021/jp909148n [PubMed: 20429599]

[250]. Genheden S Solvation free energies and partition coefficients with the coarse-grained and hybrid all-atom/coarse-grained MARTINI models. J. Comput. Aided Mol. Des, 2017, 31(10), 867–876. 10.1007/s10822-017-0059-9 [PubMed: 28875361]

[251]. Leung AKK; Hafez IM; Baoukina S; Belliveau NM; Zhigaltsev IV; Afshinmanesh E; Tieleman DP; Hansen CL; Hope MJ; Cullis PR Lipid Nanoparticles Containing siRNA Synthesized by Microfluidic Mixing Exhibit an Electron-Dense Nanostructured Core. J Phys Chem C Nanomater Interfaces, 2012, 116(34), 18440–18450. 10.1021/jp303267y [PubMed: 22962627]

[252]. Menichetti R; Kanekal KH; Kremer K; Bereau T In silico screening of drug-membrane thermodynamics reveals linear relations between bulk partitioning and the potential of mean force. J. Chem. Phys, 2017, 147(12)125101 10.1063/1.4987012 [PubMed: 28964031]

[253]. Menichetti R; Bereau T Revisiting the Meyer-Overton Rule for Drug-Membrane Permeabilities. Mol. Phys, 2019, 117, 2900–2909. 10.1080/00268976.2019.1601787

[254]. Menichetti R; Kanekal KH; Bereau T Drug-Membrane Permeability across Chemical Space. ACS Cent. Sci, 2019, 5(2), 290–298. 10.1021/acscentsci.8b00718 [PubMed: 30834317]

[255]. Aydin F; Ludford P; Dutt M Phase segregation in bio-inspired multi-component vesicles encompassing double tail phospholipid species. Soft Matter, 2014, 10(32), 6096–6108. 10.1039/C4SM00998C [PubMed: 25008809]

[256]. Li X; Tang Y-H; Liang H; Karniadakis GE Large-scale dissipative particle dynamics simulations of self-assembled amphiphilic systems. Chem. Commun. (Camb.), 2014, 50(61), 8306–8308. 10.1039/C4CC03096F [PubMed: 24938634]

[257]. Wang M; Pei S; Fang T; Yan Y; Xu J; Zhang J Dissipative Particle Dynamics Simulation on Vesicles Self-Assembly Controlled by Terminal Groups. J. Phys. Chem. B, 2018, 122(46), 10607–10614. 10.1021/acs.jpcb.8b07567 [PubMed: 30380871]

[258]. Jia L; Wang R; Fan Y Encapsulation and release of drug nanoparticles in functional polymeric vesicles. Soft Matter, 2020, 16(12), 3088–3095. 10.1039/D0SM00069H [PubMed: 32149316]

[259]. Spaeth JR; Kevrekidis IG; Panagiotopoulos AZ Dissipative particle dynamics simulations of polymer-protected nanoparticle self-assembly. J. Chem. Phys, 2011, 135(18)184903 10.1063/1.3653379 [PubMed: 22088077]

[260]. Noguchi H Dynamical Modes of Deformed Red Blood Cells and Lipid Vesicles in Flows. Prog. Theor. Phys, 2010, 184, 364–368. 10.1143/PTPS.184.364

[261]. Noguchi H; Takasu M Self-assembly of amphiphiles into vesicles: a Brownian dynamics simulation. Phys. Rev. E Stat. Nonlin. Soft Matter Phys, 2001, 64(4 Pt 1)041913 10.1103/PhysRevE.64.041913 [PubMed: 11690058]

[262]. Noguchi H; Takasu M Fusion Pathways of Vesicles: A Brownian Dynamics Simulation. J. Chem. Phys, 2001, 115, 9547–9551. 10.1063/1.1414314

[263]. Le T; Epa VC; Burden FR; Winkler DA Quantitative structure-property relationship modeling of diverse materials properties. Chem. Rev, 2012, 112(5), 2889–2919. 10.1021/cr200066h [PubMed: 22251444]

[264]. Le TC; Tran N Using Machine Learning To Predict the Self-Assembled Nanostructures of Monoolein and Phytantriol as a Function of Temperature and Fatty Acid Additives for Effective Lipid-Based Delivery Systems. ACS Appl. Nano Mater, 2019, 2, 1637–1647. 10.1021/acsanm.9b00075

[265]. Tran N; Mulet X; Hawley AM; Fong C; Zhai J; Le TC; Ratcliffe J; Drummond CJ Manipulating the Ordered Nanostructure of Self-Assembled Monoolein and Phytantriol Nanoparticles with Unsaturated Fatty Acids. Langmuir, 2018, 34(8), 2764–2773. 10.1021/acs.langmuir.7b03541 [PubMed: 29381863]

[266]. Tran N; Hawley AM; Zhai J; Muir BW; Fong C; Drummond CJ; Mulet X High-Throughput Screening of Saturated Fatty Acid Influence on Nanostructure of Lyotropic Liquid Crystalline Lipid Nanoparticles. Langmuir, 2016, 32(18), 4509–4520. 10.1021/acs.langmuir.5b03769 [PubMed: 27023315]

[267]. Speck-Planche A; Kleandrova VV; Luan F; Cordeiro MN; Computational Modeling MN Computational modeling in nanomedicine: prediction of multiple antibacterial profiles of nanoparticles using a quantitative structure-activity relationship perturbation model. Nanomedicine (Lond.), 2015, 10(2), 193–204. 10.2217/nnm.14.96 [PubMed: 25600965]

[268]. Concu R; Kleandrova VV; Speck-Planche A; Cordeiro MNDS Probing the toxicity of nanoparticles: a unified *in silico* machine learning model based on perturbation theory. Nanotoxicology, 2017, 11(7), 891–906. 10.1080/17435390.2017.1379567 [PubMed: 28937298]

[269]. Luan F; Kleandrova VV; González-Díaz H; Ruso JM; Melo A; Speck-Planche A; Cordeiro MNDS Computer-aided nanotoxicology: assessing cytotoxicity of nanoparticles under diverse experimental conditions by using a novel QSTR-perturbation approach. Nanoscale, 2014, 6(18), 10623–10630. 10.1039/C4NR01285B [PubMed: 25083742]

[270]. González-Díaz H; Arrasate S; Gómez-SanJuan A; Sotomayor N; Lete E; Besada-Porto L; Ruso JM General theory for multiple input-output perturbations in complex molecular systems. 1. Linear QSPR electronegativity models in physical, organic, and medicinal chemistry. Curr. Top. Med. Chem, 2013, 13(14), 1713–1741. 10.2174/1568026611313140011 [PubMed: 23889050]

[271]. Santana R; Zuluaga R; Gañán P; Arrasate S; Onieva E; González-Díaz H Designing nanoparticle release systems for drug-vitamin cancer co-therapy with multiplicative perturbation-theory machine learning (PTML) models. Nanoscale, 2019, 11(45), 21811–21823. 10.1039/C9NR05070A [PubMed: 31691701]

[272]. Santana R; Zuluaga R; Gañán P; Arrasate S; Onieva E; González-Díaz H Predicting coated-nanoparticle drug release systems with perturbation-theory machine learning (PTML) models. Nanoscale, 2020, 12(25), 13471–13483. 10.1039/D0NR01849J [PubMed: 32613998]

[273]. Yamankurt G; Berns EJ; Xue A; Lee A; Bagheri N; Mrksich M; Mirkin CA Exploration of the nanomedicine-design space with high-throughput screening and machine learning. Nat. Biomed. Eng, 2019, 3(4), 318–327. 10.1038/s41551-019-0351-1 [PubMed: 30952978]

[274]. Jones DE; Ghandehari H; Facelli JC A review of the applications of data mining and machine learning for the prediction of biomedical properties of nanoparticles. Comput. Methods Programs Biomed, 2016, 132, 93–103. 10.1016/j.cmpb.2016.04.025 [PubMed: 27282231]

[275]. Epa VC; Burden FR; Tassa C; Weissleder R; Shaw S; Winkler DA Modeling biological activities of nanoparticles. Nano Lett, 2012, 12(11), 5808–5812. 10.1021/nl303144k [PubMed: 23039907]

[276]. Metwally AA; Hathout RM Computer-Assisted Drug Formulation Design: Novel Approach in Drug Delivery. Mol. Pharm, 2015, 12(8), 2800–2810. 10.1021/mp500740d [PubMed: 26107396]

[277]. Hathout RM; Metwally AA Towards better modelling of drug-loading in solid lipid nanoparticles: Molecular dynamics, docking experiments and Gaussian Processes machine learning. Eur. J. Pharm. Biopharm, 2016, 108, 262–268. 10.1016/j.ejpb.2016.07.019 [PubMed: 27449631]

[278]. Metwally AA; Hathout RM Replacing Microemulsion Formulations Experimental Solubility Studies with In-Silico Methods Comprising Molecular Dynamics and Docking Experiments. Chem. Eng. Res. Des, 2015, 104, 453–456. 10.1016/j.cherd.2015.09.003

[279]. Uttarwar RG; Potoff J; Huang Y Study on Interfacial Interaction between Polymer and Nanoparticle in a Nanocoating Matrix: A MARTINI Coarse-Graining Method. Ind. Eng. Chem. Res, 2013, 52, 73–82. 10.1021/ie301228f

[280]. Saunders L; Perrin J; Gammack D Ultrasonic irradiation of some phospholipid sols. J. Pharm. Pharmacol, 1962, 14, 567–572. 10.1111/j.2042-7158.1962.tb11141.x [PubMed: 14497533]

[281]. Hargreaves WR; Deamer DW Liposomes from ionic, single-chain amphiphiles. Biochemistry, 1978, 17(18), 3759–3768. 10.1021/bi00611a014 [PubMed: 698196]

[282]. Parente RA; Lentz BR Phase behavior of large unilamellar vesicles composed of synthetic phospholipids. Biochemistry, 1984, 23(11), 2353–2362. 10.1021/bi00306a005 [PubMed: 6477871]

[283]. Song H; Geng H; Ruan J; Wang K; Bao C; Wang J; Peng X; Zhang X; Cui D Development of Polysorbate 80/Phospholipid mixed micellar formation for docetaxel and assessment of its *in vivo* distribution in animal models. Nanoscale Res. Lett, 2011, 6(1), 354. 10.1186/1556-276X-6-354 [PubMed: 21711889]

[284]. Stano P; Bufali S; Pisano C; Bucci F; Barbarino M; Santaniello M; Carminati P; Luisi PL Novel camptothecin analogue (gimatecan)-containing liposomes prepared by the ethanol injection method. J. Liposome Res, 2004, 14(1–2), 87–109. 10.1081/LPR-120039794 [PubMed: 15461935]

[285]. Ohsawa T; Miura H; Harada K Improvement of encapsulation efficiency of water-soluble drugs in liposomes formed by the freeze-thawing method. Chem. Pharm. Bull. (Tokyo), 1985, 33(9), 3945–3952. 10.1248/cpb.33.3945 [PubMed: 4092294]

[286]. Liu L; Yonetani T Preparation and characterization of liposome-encapsulated haemoglobin by a freeze-thaw method. J. Microencapsul, 1994, 11(4), 409–421. 10.3109/02652049409034258 [PubMed: 7931940]

[287]. Schieren H; Rudolph S; Finkelstein M; Coleman P; Weissmann G Comparison of large unilamellar vesicles prepared by a petroleum ether vaporization method with multilamellar vesicles: ESR, diffusion and entrapment analyses. Biochim. Biophys. Acta, 1978, 542(1), 137–153. 10.1016/0304-4165(78)90240-4 [PubMed: 208648]

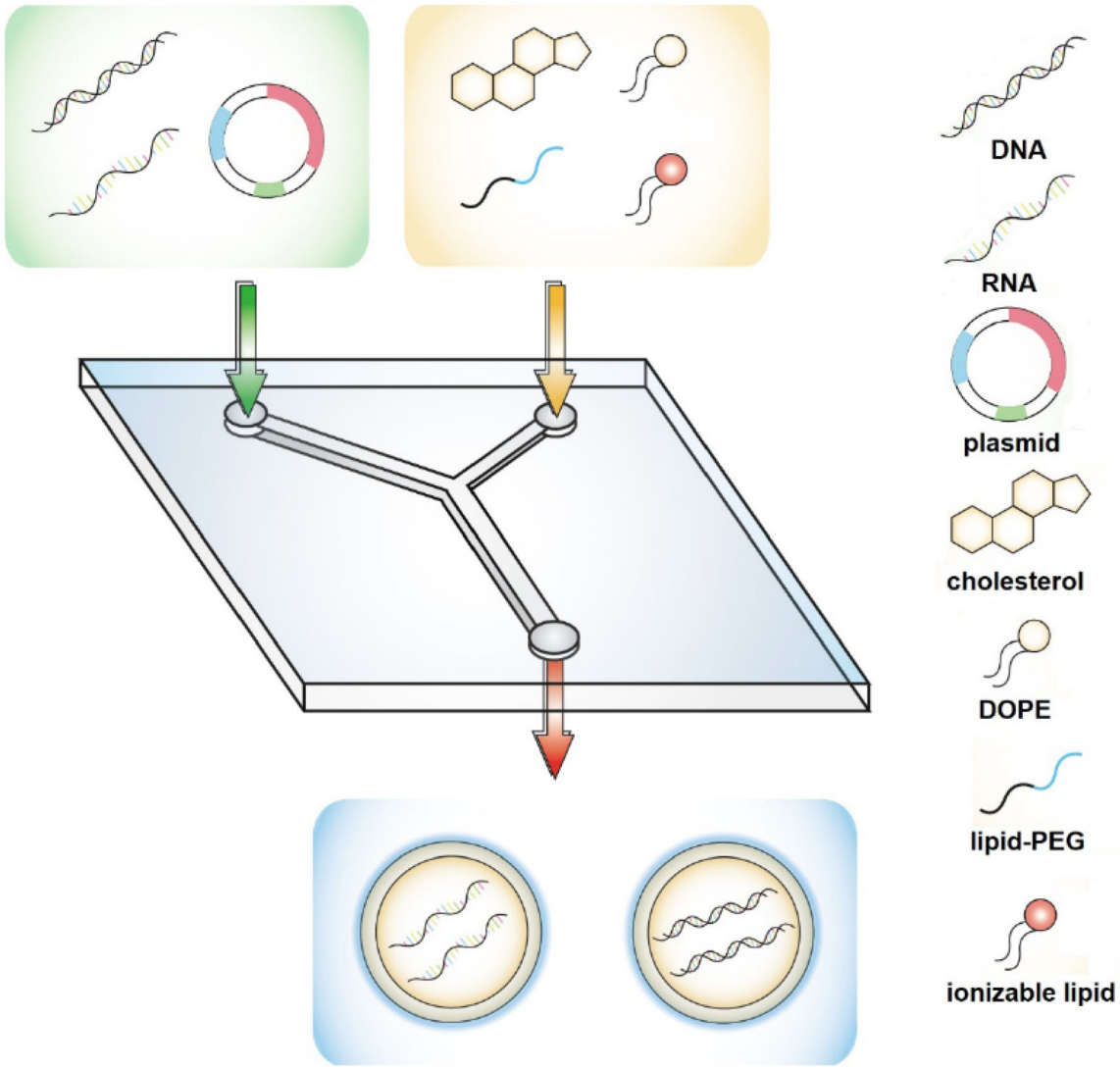

Fig. (1).
Schematic illustration of a microfluidic method for the preparation of LNPs.

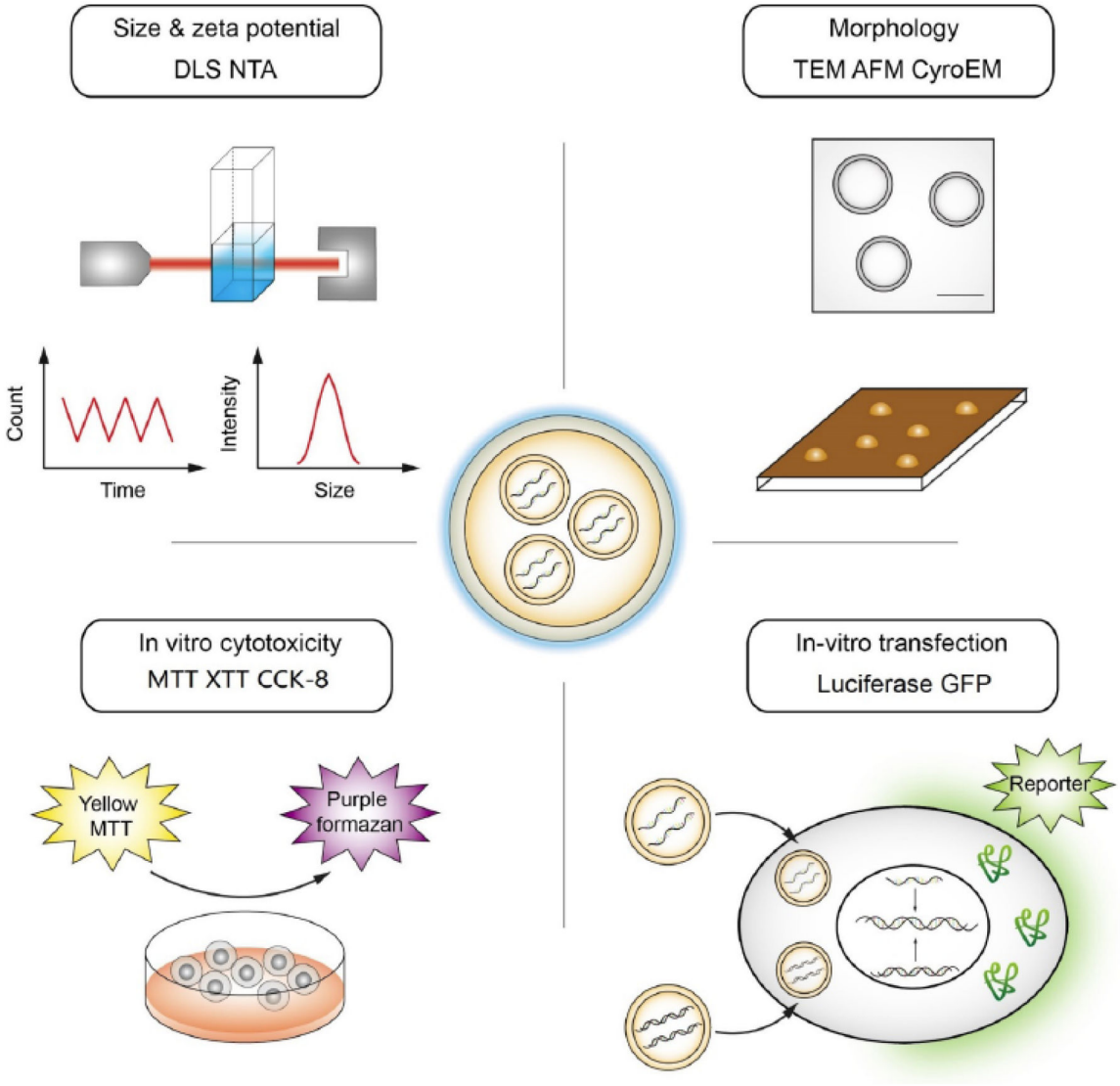

Fig. (2).
Physicochemical characterization of LNPs and representative bioassays.

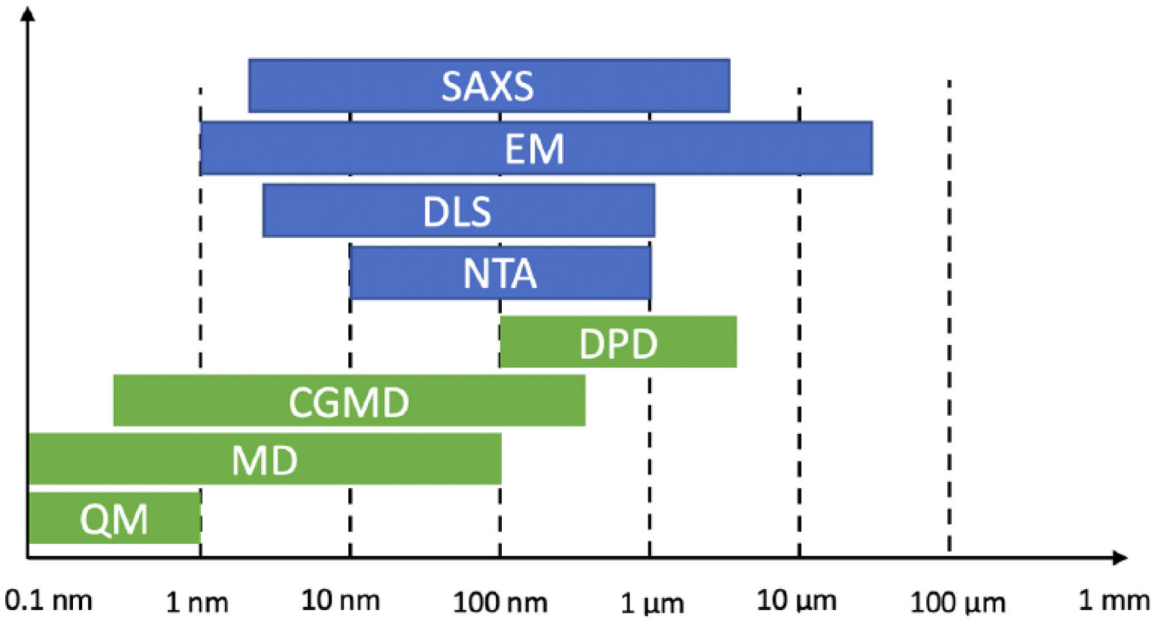

Fig. (3).
Length scales of various imaging and simulation techniques for probing LNPs.

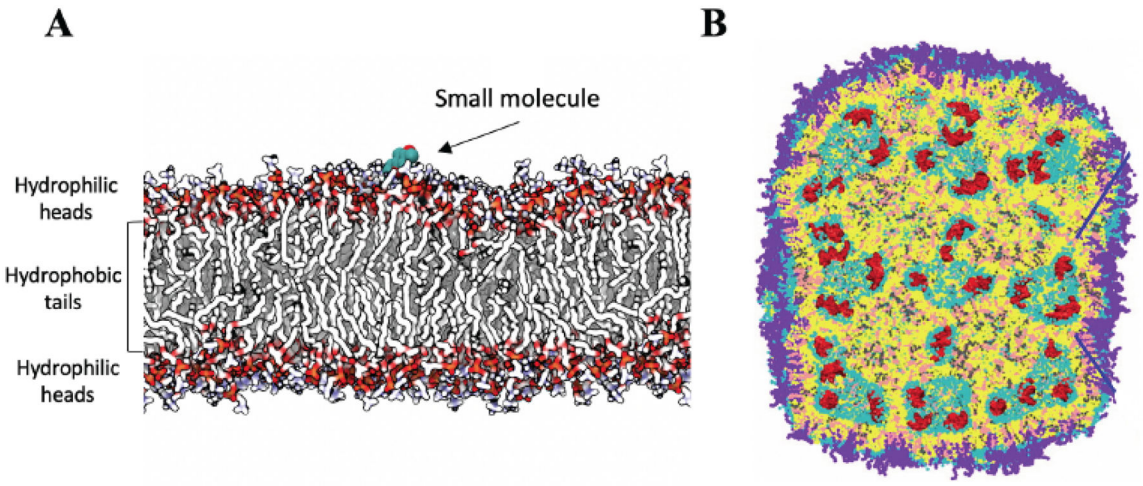

Fig. (4). A molecular view of lipid nanoparticles.

(**A**) Small molecule interacting with a lipid bilayer in an atomistic simulation. Head group oxygen and nitrogen atoms are colored in red and blue. Carbon atoms are colored in white. The small molecules shown as spheres partially partitioned in the head group region. (**B**) Coarse-grained model of LNPs used for gene delivery, composed of ionizable lipids (yellow), cholesterol (pink), phospholipid (grey; lipid polar moiety in cyan), PEG-lipid (violet), and 12 bp DNA (red). Adapted with permission from [251]. Copyright (2012–2013) American Chemical Society.

Table 1.

Overview of the characteristics of conventional preparation methods.

Preparation Method	Type of Liposomes	Particle Size (nm)	Applicable Drugs	References
Lipid film hydration	MLV	100–300	Hydrophobic drug	[93]
Thin-film sonication	SUV	20–50	Hydrophobic drug	[280–282]
French method	SUV	30–50	Hydrophobic drug	[283]
Ethanol injection	SUV	30–110	Hydrophobic drug	[284]
Freezing thawing	LUV	20–200	Hydrophilic drug	[95,285,286]
Ether injection	LUV	70–200	Hydrophilic drug	[106,287]
Reverse phase evaporation	LUV	200–1000	Hydrophilic drug	[91]